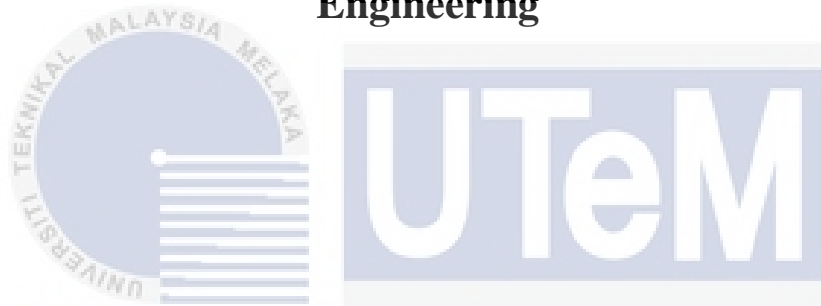




**Faculty of Electronics and Computer Technology and
Engineering**



**DEVELOPMENT OF A REFRACTIVE INDEX SENSOR BASED ON
CHANGES IN THE RADIUS OF A U-SHAPED PLASTIC OPTICAL
FIBER**

SARVINA A/P MATHIALAKAN

**Bachelor of Electronics Engineering Technology (Industrial Electronics) with
Honours**

2024

**DEVELOPMENT OF A REFRACTIVE INDEX SENSOR BASED ON CHANGES
IN THE RADIUS OF A U-SHAPED PLASTIC OPTICAL FIBER**

SARVINA A/P MATHIALAKAN

**A project report submitted
in partial fulfillment of the requirements for the degree of
Bachelor of Electronics Engineering Technology (Industrial Electronics) with
Honours**



**UNIVERSITI TEKNIKAL MALAYSIA MELAKA
Faculty of Electronics and Computer Technology and Engineering**

UNIVERSITI TEKNIKAL MALAYSIA MELAKA

2024

BORANG PENGESAHAN STATUS LAPORAN
PROJEK SARJANA MUDA II

Tajuk Projek : DEVELOPMENT OF A REFRACTIVE INDEX SENSOR BASED ON
CHANGES IN THE RADIUS OF A U-SHAPED PLASTIC OPTICAL FIBER

Sesi Pengajian : 2023/2024

Saya Sarvina A/P Mathialakan mengaku membenarkan laporan Projek Sarjana
Muda ini disimpan di Perpustakaan dengan syarat-syarat kegunaan seperti berikut:

1. Laporan adalah hak milik Universiti Teknikal Malaysia Melaka.
2. Perpustakaan dibenarkan membuat salinan untuk tujuan pengajian sahaja.
3. Perpustakaan dibenarkan membuat salinan laporan ini sebagai bahan pertukaran antara institusi pengajian tinggi.
4. Sila tandakan (✓)

SULIT*

(Mengandungi maklumat yang berdarjah keselamatan atau kepentingan Malaysia seperti yang termaktub di dalam AKTA RAHSIA RASMI 1972)

TERHAD*

(Mengandungi maklumat terhadap yang telah ditentukan oleh organisasi/badan di mana penyelidikan dijalankan)

Disahkan oleh:

TIDAK TERHAD



(TANDATANGAN PENULIS)

Alamat Tetap: No 888 Jalan Buloh Kasap
85000, Segamat, Johor.



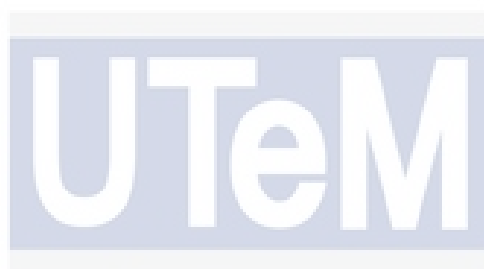
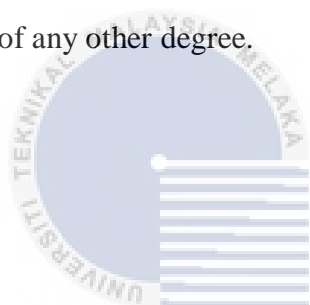
(COP DAN TANDATANGAN PENYELIA)

Tarikh: 10/1/2024

Tarikh: 10/1/2024

DECLARATION

I declare that this project report entitled “DEVELOPMENT OF A REFRACTIVE INDEX SENSOR BASED ON CHANGES IN THE RADIUS OF A U-SHAPED PLASTIC OPTICAL FIBER” is the result of my own research except as cited in the references. The project report has not been accepted for any degree and is not concurrently submitted in candidature of any other degree.



Signature

اونيور سیتی تیکنیکل ملیسیا مالاکا : 

Student Name : SARVINA A/P MATHIALAKAN

Date : 10 JANUARY 2024

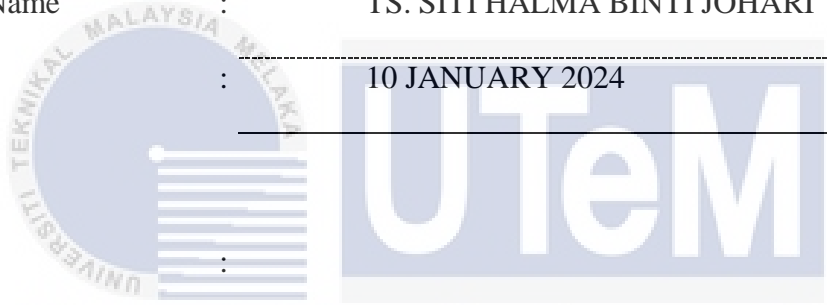
APPROVAL

I hereby declare that I have checked this project report and in my opinion, this project report is adequate in terms of scope and quality for the award of the degree of Bachelor of Electronics Engineering Technology (Industrial Electronics) with Honours.

Signature : 

Supervisor Name : TS. SITI HALMA BINTI JOHARI

Date : 10 JANUARY 2024

Signature : 

Co - Supervisor Name (if-any) : 

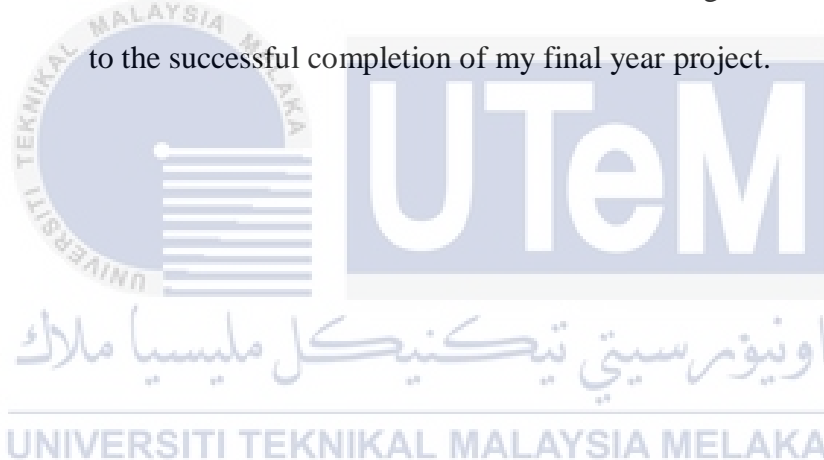
Date : 

DEDICATION

I extend this project report's dedication to my family and friends, with a special acknowledgment to my parents who instilled in me the valuable lesson that even seemingly challenging tasks can be accomplished through a step-by-step approach. Furthermore, I dedicate this work to my friends who played a crucial role in supporting and enabling me to complete the project. I am deeply grateful for the assistance and guidance received.

Additionally, I express my gratitude to my PSM Supervisor,

Ts. Siti Halma Binti Johari, for his valuable advice that significantly contributed to the successful completion of my final year project.



ABSTRACT

The refractive index, is a fundamental property of a material that describes the extent to which light is bent or refracted when it passes through it. It is defined as the ratio of the speed of light in a vacuum to the speed of light in the material. Each material has its own specific refractive index, which influences the behavior of light as it enters or travels through the material. To shows the refractive index variations, the amount of water vapor present in the air was detected using humidity sensing. Besides, humidity sensing plays a vital role in various industries, including agriculture, engineering, medicine, and more. Plastic optical fibers (POF) can be utilized as humidity sensors by tapering it manually using sandpaper, with different waist diameters such as 500 μm and 600 μm . The aim of this project is to validate the effect of evanescent wave on a U-shaped tapered POF relying on modulated light intensity to sense humidity in 3cm, 4cm and 5cm in radius. Three different wavelengths which are 470 nm, 530 nm, and 645 nm were used to evaluate the sensor's sensitivity in range of 35% RH to 90% RH of humidity level. The sensor was expected to demonstrate on inversely proportional to RH level. Data analysis included parameters such as trendline and sensitivity.

Keywords: Plastic optical fiber, Evanescent wave, Humidity, Refractive index sensor and U-Shaped.

ABSTRAK

Indeks biasan, ialah sifat asas sesuatu bahan yang menerangkan sejauh mana cahaya dibengkokkan atau dibiaskan apabila ia melaluinya. Ia ditakrifkan sebagai nisbah kelajuan cahaya dalam vakum kepada kelajuan cahaya dalam bahan. Setiap bahan mempunyai indeks biasannya sendiri, yang mempengaruhi tingkah laku cahaya semasa ia memasuki atau bergerak melalui bahan. Untuk menunjukkan variasi indeks biasan, jumlah wap air yang terdapat di udara telah dikesan menggunakan penderiaan kelembapan. Selain itu, penderiaan kelembapan memainkan peranan penting dalam pelbagai industri, termasuk pertanian, kejuruteraan, perubatan dan banyak lagi. Gentian optik plastik (POF) boleh digunakan sebagai penderia kelembapan dengan mengetuknya secara manual menggunakan kertas pasir, dengan diameter pinggang yang berbeza seperti 500 μm dan 600 μm . Matlamat projek ini adalah untuk mengesahkan kesan gelombang evanescent pada POF tirus berbentuk U bergantung pada keamatan cahaya termodulat untuk merasakan kelembapan dalam radius 3cm, 4cm dan 5cm. Tiga panjang gelombang yang berbeza iaitu 470 nm, 530 nm, dan 645 nm telah digunakan untuk menilai sensitiviti sensor dalam julat 35% RH hingga 90% RH tahap kelembapan. Penderia dijangka menunjukkan berkadar songsang dengan tahap RH. Analisis data termasuk parameter seperti garis arah aliran dan sensitiviti.

Kata kunci: Gentian optik plastik, Gelombang Evanescent, Kelembapan, Penderia indeks biasan dan Berbentuk U.

TABLE OF CONTENTS

ABSTRACT	vi
ABSTRAK	vii
TABLE OF CONTENTS	viii
LIST OF FIGURES	xii
LIST OF TABLES	xv
CHAPTER 1 INTRODUCTION	1
1.1 Background	1
1.2 Problem Statement	1
1.3 Project Objective	2
1.4 Scope of Project	2
CHAPTER 2 LITERATURE REVIEW	3
2.1 Introduction	3
2.2 Fiber Optic	3
2.2.1 Single Mode	5
2.2.2 Multimode	7
2.2.3 Propagation of Light among a fiber	9
2.2.4 Reflective and Refractive	11
2.2.5 Numerical Aperture	12
2.3 A Related Previous Work	14

- 2.3.1 “Enhance sensitivity of plastic optical fiber sensor by spiral configuration for body temperature applications” by A Arifin, K R Amaliyah, A K Lebang, N Hamrun, S Dewang, and D Tahir (2020). 14
- 2.3.2 “Intensity Modulation based U shaped Plastic Optical Fiber Refractive Index Sensor,” by J. J. Patil and A. Ghosh, 15
- 2.3.3 “Refractive Index Sensor Based on Double Side-Polished U-Shaped Plastic Optical Fiber” by Shumin Wang, Daming Zhang, Yan Xu, Siwen Sun and Xiaoqiang Sun. 16
- 2.3.4 “Double-side polished U-shape plastic optical fiber based SPR sensor for the simultaneous measurement of refractive index and temperature” by Chuanxin Teng, Peng Shao, Shiwei Li, Shu Li, Houquan Liu, Hongchang Deng, Ming Chen, Libo Yuan, Shijie Deng. 16
- 2.3.5 “All Plastic Optical Fiber-based Respiration Monitoring Sensor” by Wern Kam, Waleed S. Mohammed, Gabriel Leen, Kieran O’ Sullivan, Mary O’Keeffe, Sinead O’Keeffe and Elfed Lewis (2017). 17
- 2.3.6 “Parallel Polished Plastic Optical Fiber-Based SPR Sensor for Simultaneous Measurement of RI and Temperature” by Lian Liu, Jie Zheng, Shijie Deng, Libo Yuan and Chuanxin Teng (2021). 18
- 2.3.7 "U-Shaped Plastic Fiber Optic Sensor for Measuring Adulteration in Liquids via RGB Color Changes," by J. D. Filoteo-Razo et al. 18
- 2.3.8 “Humidity and Isopropyl Alcohol Detection Sensor Based on Plastic Optical Fiber” by Lorant A. Szolga (2021). 19

2.3.9	“Fiber optic sensors based on circular and elliptical polymer optical fiber for measuring refractive index of liquids” by Fei Ye, Cui Tian, Cuihua Ma, Zhi Feng Zhang	20
2.3.10	“Intensity-Modulated Polymer Optical Fiber-Based Refractive Index Sensor” by Chuanxin Teng , Rui Min , Jie Zheng , Shijie Deng , Maosen Li , Li Hou and Libo Yuan.	21
2.4	Summary of literature	23
2.5	Hardware Implementation	24
2.5.1	Light Emitting Diode (LED)	24
2.5.2	Phototransistors	24
2.5.3	Digital Humidity Temperature Meter	25
2.5.4	Amplifier Circuit	26
2.5.5	Plastic Optical Fiber Sensor	26
2.5.6	NodeMCU	27
2.6	Summary	28
CHAPTER 3 METHODOLOGY		29
3.1	Introduction	29
3.2	Methodology	29
3.2.1	Flowchart	30
3.2.2	Fabrication of Tapered Plastic Optical Fiber (POF)	31
3.3	Experimental Setup	34
3.4	Summary	39
CHAPTER 4 RESULTS AND DISCUSSIONS		40

4.1	Introduction	40
4.2	Results and Analysis	40
4.2.1	Repeatability Test	40
4.2.1.1	Red (645 nm)	41
4.2.1.2	Green (530 nm)	44
4.2.1.3	Blue (470 nm)	48
4.2.2	Trendline	51
4.2.3	Hysteresis	60
4.3	Summary	61
	CHAPTER 5 CONCLUSION AND RECOMMENDATIONS	62
5.1	Conclusion	62
5.2	Future Works	63
	REFERENCES	64



LIST OF FIGURES

FIGURE	TITLE	PAGE
Figure 2.1	Structure of Fiber Optic.	4
Figure 2.2	Difference between Multimode fiber and single mode fiber.	9
Figure 2.3	The light propagation in optical fiber.	11
Figure 2.4	Total Internal Reflection.	12
Figure 2.5	Numerical aperture of optical fiber	13
Figure 2.6	The way light enters and propagates through an optical fiber core.	13
Figure 2.7	Light Emitting Diode (LED).	24
Figure 2.8	Phototransistors.	25
Figure 2.9	Digital Humidity Temperature Meter	25
Figure 2.10	Amplifier circuit.	26
Figure 2.11	Plastic Optical Fiber Sensor.	27
Figure 2.12	NodeMCU.	27
Figure 3.1	Flowchart of the project	30
Figure 3.2	Plastic Optical Fiber	31

Figure 3.3 Fiber optic and wire stripper, POF cutter and ruler.	31
Figure 3.4 POF cable after the middle is cut.	32
Figure 3.5 POF cable after the middle is cut.	33
Figure 3.6 Thickness of POF cable.	33
Figure 3.7 Digital micrometer	33
Figure 3.8 shows the measurement of stripped area.	34
Figure 3.9 Shows the LED light (a) and tape (b).	34
Figure 3.10 Solder the container to make the hole.	35
Figure 3.11 Adjusting the item's component and	36
Figure 3.12 Shows the hardware components: (a) amplifier circuit, (b) digital humidity temperature, (c) battery, (d) LED light and phototransistor, (e) Component arrangement, and (f) Experimental setup.	38
Figure 4.1 The repeatability test of (a) 500 μm (3cm), (b) 500 μm (4cm), (c) 500 μm (5cm) , (d) 600 μm (3cm), (e) 600 μm (4cm) and (f) 600 μm (5cm) for red wavelength.	43
Figure 4.2 The repeatability test of (a) 500 μm (3cm), (b) 500 μm (4cm), (c) 500 μm (5cm) , (d) 600 μm (3cm), (e) 600 μm (4cm) and (f) 600 μm (5cm) for green wavelength.	47

Figure 4.3 The repeatability test of (a) 500 μm (3cm), (b) 500 μm (4cm), (c) 500 μm (5cm) , (d) 600 μm (3cm), (e) 600 μm (4cm) and (f) 600 μm (5cm) for blue wavelength.	50
Figure 4.4 Trendline graph for the red wavelength.	52
Figure 4.5 Trendline graph for the green wavelength.	53
Figure 4.6 Trendline graph for the blue wavelength.	54
Figure 4.7 Hysteresis for the 500 μm waist diameter of red wavelength	60



LIST OF TABLES

TABLE	TITLE	PAGE
Table 4.1	The characteristics of a U-shaped	55
Table 4.2	The characteristics of a U-shaped tapered POF for the red wavelength for 4cm.	55
Table 4.3	The characteristics of a U-shaped tapered POF for the red wavelength for 5cm.	56
Table 4.4	The characteristics of a U-shaped tapered POF for the green wavelength.	56
Table 4.5	The characteristics of a U-shaped tapered POF for the green wavelength.	57
Table 4.6	The characteristics of a U-shaped tapered POF for the green wavelength.	57
Table 4.7	Characteristics of a U-shaped tapered POF for the blue wavelength.	58
Table 4.8	Characteristics of a U-shaped tapered POF for the blue wavelength.	58
Table 4.9	Characteristics of a U-shaped tapered POF for the blue wavelength.	58
Table 4.10	Characteristics of a U-shaped tapered POF for 500um at all wavelength.	59

CHAPTER 1

INTRODUCTION

1.1 Background

Plastic optical fiber, also called polymer optical fiber or POF, is a plastic-based fiber. It typically employs fluorinated polymers for cladding and PMMA (acrylic) for the core, enabling effective light transmission (up to 96% in a 1 mm diameter fiber). Plastic optical fiber emits harmless green or red light that can be seen by humans. Compared to glass fiber, plastic optical fiber is known for its flexibility and durability[1]. Polymer optical fibers (POFs) based SPR sensors have a lot of achievable in biosensing fields because of their specific merits of good flexibility, high coupling efficiency and convenient fabrication[2].

1.2 Problem Statement

Recent advancements in technology have enabled the development of lightweight and portable equipment. However, the experimental setup poses a challenge. Due to its hard structure and strength, silica glass is more likely to break than Plastic Optical Fiber (POF). POF is less likely to break since it is a polymer, which is more elastic and flexible. Silica is more fragile due to its higher hardness and stiffness, as well as the manufacturing method.

1.3 Project Objective

- a. To develop circuits for LED light sources and phototransistors using Microcontroller.
- b. To fabricate a tapered POF with 500 μm and 600 μm waist diameter.
- c. To validate experimentally the tapered POF with different bent radius and wavelength towards humidity sensing application.

1.4 Scope of Project

The primary objective of this project is to utilize a U-shaped tapered Plastic Optical Fiber (POF) with specific parameters, including taper waist diameter, taper length, and bend radius, to accurately measure humidity levels. The polished POF samples were prepared with waist diameters of 500 μm and 600 μm . The taper length was set at 3 cm, and the fiber was bent into a radius of 3 cm, 4 cm, and 5 cm. The light source used for the experiments consisted of LEDs with wavelengths of 470 nm (blue), 530 nm (green), and 645 nm (red). The POF samples were exposed to relative humidity (RH) ranging from 35% to 90%. The output measurement for assessing the sensor's performance is voltage (V). Key qualities evaluated for the sensor include sensitivity, linearity, average standard deviation, and resolution. The focus of the application is on measuring relative humidity.

CHAPTER 2

LITERATURE REVIEW

2.1 Introduction

This chapter will discuss the journal, researcher, and article related to similar projects, previous analyses, and comparisons of methodologies, analyses, and approaches. It aims to provide a comprehensive overview of plastic optical fiber sensors and their applications in humidity sensing.

2.2 Fiber Optic

Fiber optics refers to a technology that utilizes thin strands of glass or plastic called optical fibers to transmit light signals over long distances and at high speeds. These optical fibers are designed to carry optical signals in the form of light pulses, which can transmit vast amounts of data over significant distances with minimal loss and interference. The structure of a fiber optic cable typically consists of three primary components:

- i. Core: The core is the central part of the optical fiber through which light signals travel. It is usually made of high-purity glass or plastic material and has a very small diameter, typically around 9 to 125 micrometers. The core is designed to guide and transmit light signals along its length through a process called total internal reflection.
- ii. Cladding: Surrounding the core is the cladding, which is made of a material with a lower refractive index than the core. The cladding helps to confine the light within the core by reflecting the light back into the core through total internal

reflection[3]. This prevents the light from escaping or being absorbed by the surroundings, thus maintaining signal integrity.

- iii. **Buffer/Coating:** The outermost layer of the fiber optic cable is the buffer or coating, which serves as a protective layer for the fiber. It provides mechanical strength, insulation, and resistance to environmental factors such as moisture, temperature, and abrasion. The buffer can be made of materials like acrylate, silicone, or polyimide, depending on the specific application and environment.

The fundamental principle of fiber optics relies on the principle of total internal reflection. When light enters the core of the optical fiber at a certain angle, it undergoes multiple internal reflections within the core, bouncing off the cladding. This continuous reflection allows the light to travel through the fiber with minimal loss and without significant degradation. Glass fiber offers some benefits as a tiny tube, including superior flexibility, ease of production, long length, and electromagnetic field immunity[4].

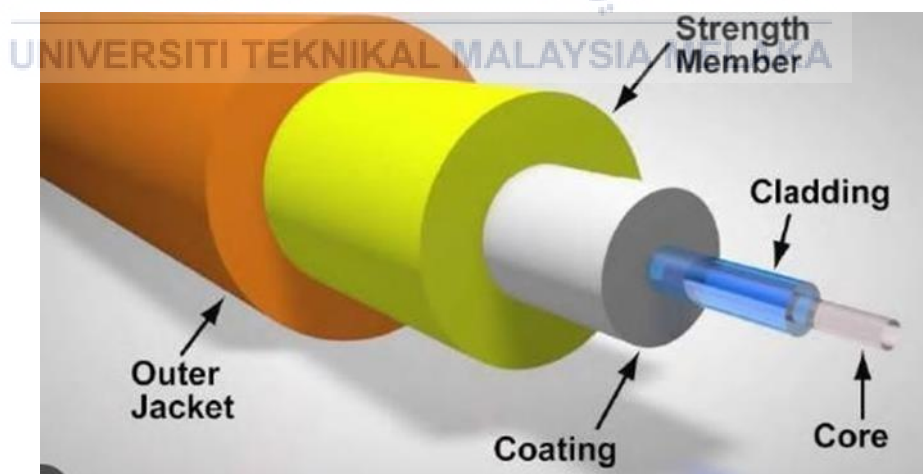


Figure 2.1 Structure of Fiber Optic.

2.2.1 Single Mode

Single-mode fiber optic refers to a type of optical fiber that allows the transmission of a single mode or path of light at a time. Unlike multimode fiber, which supports multiple light modes, single-mode fiber has a smaller core diameter and is designed to propagate a single mode of light with high fidelity over long distances[5].

In single-mode fiber, the core diameter is typically around 8 to 10 micrometers, much smaller than the core diameter of multimode fiber. This small core size enables the transmission of light in a single mode, which reduces the occurrence of modal dispersion and allows for higher data rates and longer transmission distances.

The concept of single-mode transmission is based on the principle of total internal reflection, like multimode fiber. However, due to the smaller core size, single-mode fiber restricts light propagation to a narrow beam, resulting in a more direct and focused light path. This minimizes the dispersion of the transmitted light pulses and reduces signal degradation, enabling single-mode fiber to achieve higher bandwidth and longer transmission distances compared to multimode fiber. Single-mode fiber optics offer several advantages and applications:

- **Longer Transmission Distances:** Single-mode fiber can transmit signals over much longer distances compared to multimode fiber. The reduced modal dispersion in single-mode fiber allows for higher transmission speeds and minimal signal loss, making it suitable for long-haul communications, such as telecommunication networks and undersea cables.

- **Higher Bandwidth:** Single-mode fiber provides higher bandwidth capacity compared to multimode fiber. It supports higher data rates and is commonly used in high-speed applications, such as long-distance data transmission, video streaming, and backbone networks.
- **Enhanced Signal Quality:** The narrow and focused light path in single-mode fiber minimizes signal degradation and improves signal quality. This results in lower attenuation (signal loss) and lower levels of dispersion, ensuring reliable and high-quality signal transmission.
- **Compatibility with Wavelength-Division Multiplexing (WDM):** Single-mode fiber is compatible with wavelength-division multiplexing (WDM) technology, which allows multiple wavelengths of light to be transmitted simultaneously over a single fiber. This enables the transmission of multiple independent data streams, significantly increasing the overall capacity of the fiber.

It is important to note that single-mode fiber requires more precise alignment and specialized equipment for installation and termination compared to multimode fiber. This makes it slightly more expensive and complex to work with. However, the advantages of single-mode fiber in terms of longer reach and higher bandwidth make it the preferred choice for long-haul communications and high-capacity data transmission.

The choice between single-mode and multimode fiber depends on the specific application requirements, budget constraints, and performance needs. Single-mode fiber is typically used in applications that demand high data rates, long transmission distances, and excellent signal integrity.

2.2.2 Multimode

Multimode optical fiber was the first to be created and marketed, simply referring to how many modes or light beams support each other through a waveguide at the same time. Multimode fiber optic refers to a type of optical fiber that is designed to transmit multiple light modes or paths simultaneously. In multimode fiber, the core diameter is larger compared to single-mode fiber, typically ranging from 50 to 62.5 micrometers. This larger core size allows for the propagation of multiple light modes.

The concept of multimode transmission is based on the principle of different light paths or modes traveling through the core of the fiber at slightly different angles. These modes can bounce off the walls of the core and the cladding, leading to a phenomenon known as modal dispersion. Modal dispersion is the spreading out of the light pulses as they travel through the fiber, which can limit the distance and data rates achievable in multimode fiber compared to single-mode fiber. There are two main types of multimode fiber:

- **Step-Index Multimode Fiber:** In step-index multimode fiber, the core has a uniform refractive index throughout its diameter. This means that the refractive index abruptly changes at the core-cladding interface. Step-index multimode fiber is commonly used for shorter distance applications, such as local area networks (LANs) and data centers.
- **Graded-Index Multimode Fiber:** Graded-index multimode fiber has a core with a varying refractive index, gradually decreasing from the center to the periphery. This refractive index profile helps to reduce modal dispersion by allowing the light to travel at different speeds depending on its position within the core. Graded-index multimode fiber is often used for medium-range applications, such as campus networks and video distribution.

Multimode fiber optics offer several advantages and applications[6]:

- **Cost-effectiveness:** Multimode fiber is generally more affordable compared to single-mode fiber. This makes it a cost-effective option for shorter-distance applications where the higher data rates of single-mode fiber are not necessary.
- **Ease of Installation:** The larger core size of multimode fiber makes it easier to work with during installation and termination. It allows for a wider alignment tolerance, simplifying the connectorization process.
- **Shorter Reach:** Multimode fiber is typically used for shorter distance applications, typically up to a few kilometers. It is commonly employed in LANs, building backbones, and data center interconnections.
- **Data Transmission:** Multimode fiber can support a range of data transmission rates, including Gigabit Ethernet, 10 Gigabit Ethernet, and beyond. While the maximum data rates and reach are limited compared to single-mode fiber, multimode fiber still provides ample bandwidth for many applications.

It is important to note that multimode fiber has limitations in terms of distance and achievable data rates compared to single-mode fiber. Therefore, when longer distances or higher data rates are required, single-mode fiber is typically used. The choice between multimode and single-mode fiber depends on the specific application, budget constraints, and performance requirements.

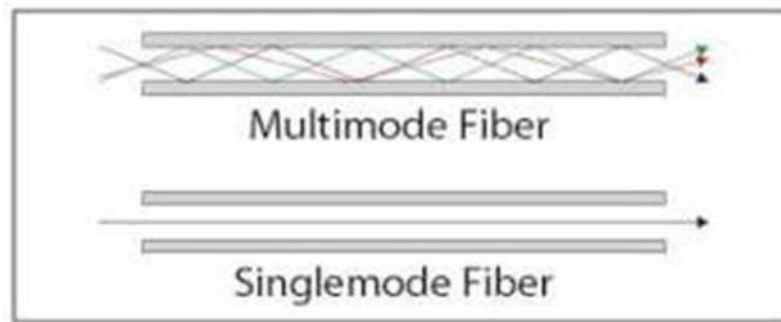


Figure 2.2 Difference between Multimode fiber and single mode fiber.

2.2.3 Propagation of Light among a fiber

The propagation of light in a fiber optic cable involves the transmission of light signals through the core of the fiber, guided by the principle of total internal reflection. In fiber optics, the information carrier is a light beam that travels at a speed of 3×10^8 ms, which is far faster and more efficient than electronics in an electric current. The core of the fiber, typically made of glass or plastic, has a higher refractive index than the surrounding cladding, which allows for the confinement and efficient transmission of light[7]. Here is a step-by-step explanation of how light propagates through a fiber optic cable:

1. **Injection of Light:** Light signals are injected into one end of the fiber optic cable using a light source, such as a laser or LED. The light travels through the core of the fiber, guided by the refractive index difference between the core and cladding.
2. **Total Internal Reflection:** As the light enters the core, it encounters the core-cladding interface. Due to the higher refractive index of the core, the light undergoes total internal reflection, meaning it reflects into the core rather than being refracted out into the cladding. This reflection occurs because the

- light hits the interface at an angle greater than the critical angle, which is determined by the refractive index difference between the core and cladding.
3. **Multiple Total Internal Reflections:** The light continues to bounce off the core-cladding interface as it propagates along the length of the fiber. Each reflection ensures that the light remains confined within the core and undergoes minimal loss or dispersion.
 4. **Single-Mode or Multimode Propagation:** Depending on the type of fiber optic cable (single- mode or multimode), the light can propagate in different ways. In single-mode fiber, the core diameter is small enough to support the transmission of a single mode of light, resulting in a tightly focused beam with minimal dispersion. In multimode fiber, the larger core diameter allows for the propagation of multiple modes, resulting in a broader beam that may experience some dispersion over long distances.
 5. **Signal Attenuation:** As the light propagates through the fiber, it experiences some attenuation, which is the gradual loss of signal strength due to factors like absorption, scattering, and bending losses. However, optical fibers are designed to minimize attenuation and allow for long-distance transmission of light signals.
 6. **Reception of Light:** At the receiving end of the fiber optic cable, a photo detector or receiver converts the transmitted light signals back into electrical signals. The receiver interprets these electrical signals and can process them further for various applications such as data transmission, telecommunications, or sensing.

The propagation of light in a fiber optic cable allows for the efficient and reliable transmission of data, voice, or video signals over long distances. The principle of total internal reflection ensures that the light remains confined within the core, minimizing signal loss and maintaining signal integrity throughout the transmission. The use of fiber optics has revolutionized telecommunications, internet connectivity, and many other fields by providing high-speed, high- bandwidth, and low-loss transmission capabilities.

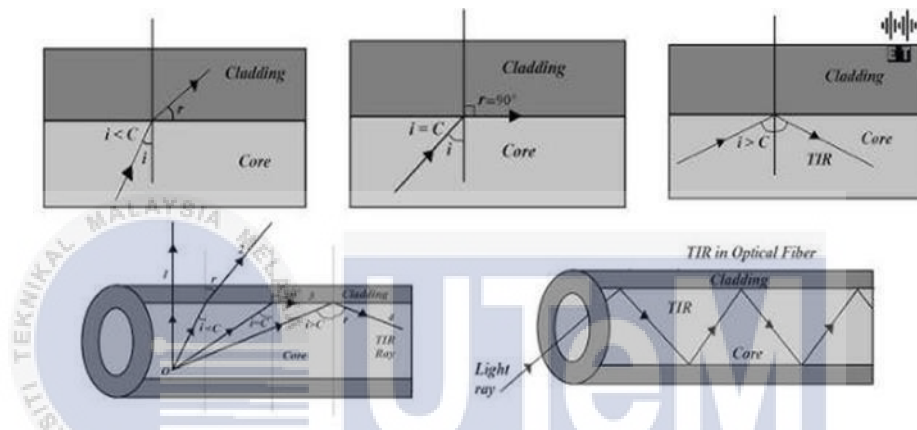


Figure 2.3 The light propagation in optical fiber.

2.2.4 Reflective and Refractive

The notion of total internal reflection is used in fiber optics to collect the transmitted light and restrict it to the fiber's core. The speed at which light travels from one material to other changes, causing the light to change direction[8]. The refractive index measurement is one of the essential components of researching materials' physical, chemical, and biological properties. The intensity of light reflected from a surface is determined by the texture of the surface and the distance between it and the light source. The refractive index of glass or other optical materials is a measurement of the speed of light in the material, and variations in the refractive index cause light to bend. According to Snell's law, as light propagates from one substance to another, the angle at which it reflects is determined by the refractive index of

the two materials (core and cladding). U-bent probes are a popular probe configuration for optical fiber sensors, known for their outstanding refractive index sensing capabilities. They offer enhanced sensitivity and accuracy due to their bent shape, which promotes efficient interaction between guided light and the surrounding medium. U-bent probes provide stability and robustness, making them suitable for practical sensor applications. Their excellent performance has made them a promising choice in optical fiber sensor research [9].

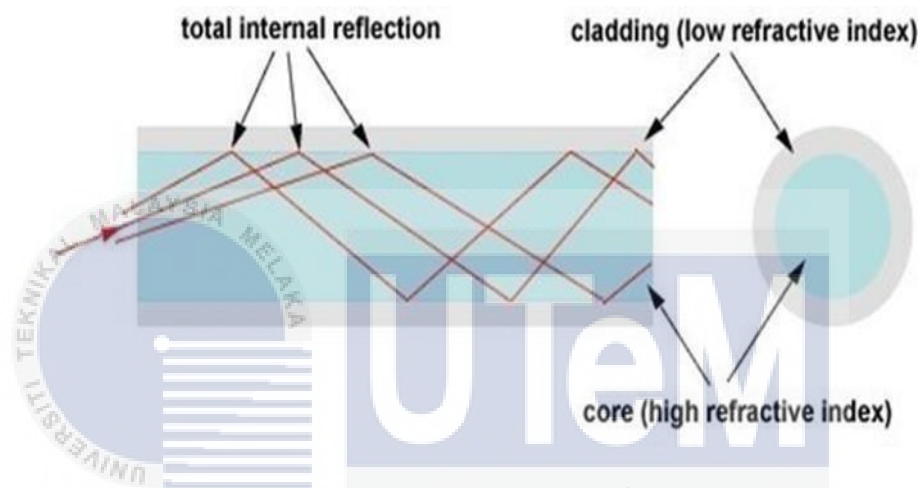
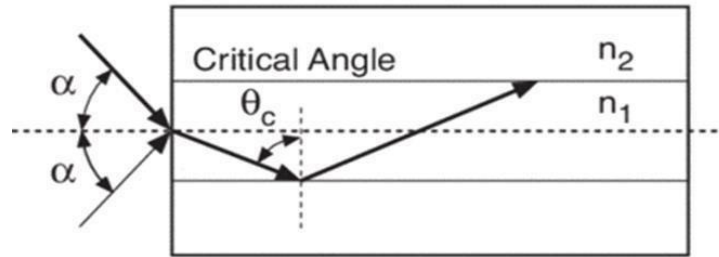


Figure 2.4 Total Internal Reflection.

2.2.5 Numerical Aperture

The light ray phenomenon inside the optic fiber core was previously explained. It is now time to grasp the concept of the amount of light that can be accepted at the optical fiber core's entrance before it can proceed into the core. The acceptance angle, often known as the maximum angle, is the angle at which something is accepted. We calculate the numerical aperture (NA), the sine of the acceptance angle, a , to determine the capacity of light acceptance. According to the formula, the difference in refractive index between the core and the cladding is what determines NA.

Numerical Aperture



$$NA = \sin \alpha = \sqrt{n_1^2 - n_2^2}$$

$$\text{Full Acceptance Angle} = 2\alpha$$

Figure 2.5 Numerical aperture of optical fiber

The equation from Figure 2.8 shows that a more considerable NA value corresponds to a larger acceptance angle, implying that more light rays are gathered. The acceptance cone or total acceptance angle will be twice as large as the acceptance angle. The efficiency of light coupling, which is occasionally necessary for implementing this technology, will benefit as the acceptance angle grows.

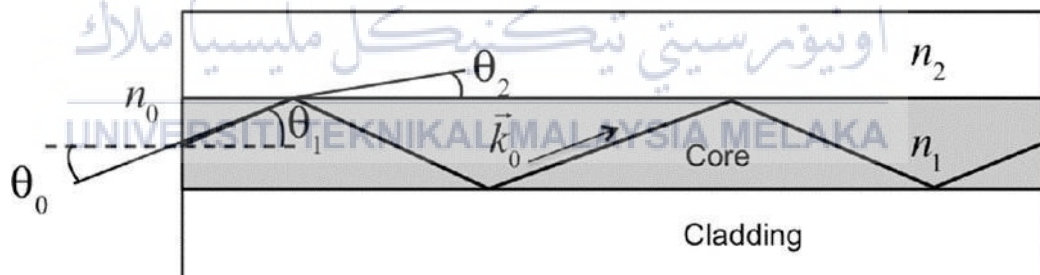


Figure 2.6 The way light enters and propagates through an optical fiber core.

Figure 2.9 shows that the medium count before entering the core was air, with $n=1$. When light strikes a core with a differing refractive index, it undergoes refraction and bends away from or toward the regular line, depending on the incidence angle. The total internal reflection (TIR) occurs in the core[10].

2.3 A Related Previous Work

2.3.1 “Enhance sensitivity of plastic optical fiber sensor by spiral configuration for body temperature applications” by A Arifin, K R Amaliyah, A K Lebang, N Hamrun, S Dewang, and D Tahir (2020).

Optical fibers have found applications in various research projects, including the use of Fiber Bragg Grating (FBG) sensors to measure body temperature in radio frequency medical therapy. However, this approach has limitations, such as high cost and low precision. To address the complexities involved in monitoring body temperature, a Mach - Zehnder interferometer is employed for temperature measurement. This method relies on a low- sensitivity Long Period Grating (LPG) optical fiber as the temperature sensor. In contrast, FBG sensors, which prioritize sensitivity, are utilized for body temperature sensing. Nonetheless, these sensors also suffer from cost and sensitivity constraints. Another study explored the use of multicore optical fibers for temperature assessment, but the methods proved to be challenging.

This journal presents the development of body temperature sensors using macro-bending analysis based on Plastic Optical Fiber (POF). The sensors form a spiral pattern as the diameter and number of bends vary. Positioned under the armpit and attached to an elastic cloth, these sensors measure body temperature. Changes in body temperature affect the light transmitted through the optical fiber sensor, resulting in power loss. The phototransistor and differential amplifier receive reduced light due to this power loss. The Arduino Uno microcontroller is employed to display the sensor's power loss and temperature measurements on a computer. The temperature range selected for the study was 28°C to 42°C. The most favorable sensor performance was observed with a spiral arrangement consisting of four bends and a diameter of 0 cm. Noteworthy results include a range of 0.421V, sensitivity of 30.071 mV/°C, and resolution of 0.033 °C. The sensor's properties

improve the spiral's diameter decreases and the number of bends increases. Utilizing POF helps enhance the temperature sensor's sensitivity. This sensor is well-suited for measuring body temperature due to its high sensitivity, cost-effectiveness, ease of manufacturing, and simplicity of measurements[11] .

2.3.2 “Intensity Modulation based U shaped Plastic Optical Fiber Refractive Index Sensor,” by J. J. Patil and A. Ghosh,

Optical fiber sensors have become increasingly important in various fields due to their ability to provide accurate and reliable measurements. This literature review examines the article titled "Intensity Modulation-based U-shaped Plastic Optical Fiber Refractive Index Sensor" by Patil and Ghosh, presented at the 2022 6th International Conference on Trends in Electronics and Informatics (ICOEI). The review aims to delve into the research conducted by the authors and provide insights into the advancements and applications of the proposed sensor. Patil and Ghosh present an innovative approach to measuring refractive index changes using an intensity modulation-based U-shaped plastic optical fiber (POF) sensor.

The authors provide a comprehensive analysis of the sensor's design, working principle, experimental setup, and performance evaluation. The literature review establishes the theoretical foundation for the research by discussing relevant concepts and technologies. It emphasizes the importance of refractive index sensing and the challenges associated with traditional methods. The authors propose an alternative approach utilizing intensity modulation and a U-shaped POF configuration to achieve accurate and cost-effective measurements. The review also discusses the fundamental principles of light propagation in optical fibers and the mechanisms involved in refractive index sensing. The article describes the design of the proposed U-shaped POF refractive index sensor and provides a detailed explanation of its working principle. The authors illustrate how changes in the surrounding

refractive index affect the light propagation through the U-shaped POF. They discuss the modulation scheme employed to generate intensity variations and the signal processing techniques used to extract precise measurements[12].

2.3.3 “Refractive Index Sensor Based on Double Side-Polished U-Shaped Plastic Optical Fiber” by Shumin Wang, Daming Zhang, Yan Xu, Siwen Sun and Xiaoqiang Sun.

The study conducted by Wang, Zhang, Xu, Sun, and Sun (2020) investigates the development of a refractive index sensor using a double side-polished U-shaped plastic optical fiber (POF). The researchers highlight the importance of refractive index sensing in various industries and discuss the advantages of using POF, such as its flexibility and ease of fabrication. They describe the experimental setup and methodology employed to evaluate the sensor's performance, focusing on sensitivity, repeatability, and stability. The obtained results demonstrate the sensor's ability to accurately detect and measure changes in refractive index. The study concludes by discussing the potential applications of the double side polished U-shaped POF sensor and its contributions to the field of optical sensing. Overall, this research provides valuable insights into the design and functionality of a cost-effective refractive index sensor based on POF[13].

2.3.4 “Double-side polished U-shape plastic optical fiber based SPR sensor for the simultaneous measurement of refractive index and temperature” by Chuanxin Teng, Peng Shao, Shiwei Li, Shu Li, Houquan Liu, Hongchang Deng, Ming Chen, Libo Yuan, Shijie Deng.

The article titled "Double-side polished U-shape plastic optical fiber based SPR sensor for the simultaneous measurement of refractive index and temperature" by Teng et al. explores the development of a U-shaped plastic optical fiber sensor for simultaneous measurement of refractive index and temperature using surface plasmon resonance (SPR)

phenomenon. The authors propose a novel sensor design that incorporates double-side polishing of the U-shaped plastic optical fiber to enhance the interaction between the fiber and the surrounding medium. By exploiting the SPR effect, the sensor can detect changes in the refractive index of the surrounding medium, providing valuable information about its composition. Additionally, the sensor design allows for the measurement of temperature variations, enabling dual parameter sensing capabilities. The article presents experimental results demonstrating the sensor's performance and discusses its potential applications in various fields. Overall, this research contributes to the advancement of U-shaped plastic optical fiber sensors for multifunctional sensing applications involving refractive index and temperature measurements[14].

2.3.5 “All Plastic Optical Fiber-based Respiration Monitoring Sensor” by Wern Kam, Waleed S. Mohammed, Gabriel Leen, Kieran O’ Sullivan, Mary O’Keeffe, Sinead O’Keeffe and Elfed Lewis (2017).

A breathing-condition monitor was developed using a fluorescent plastic optical fiber as a humidity sensor to detect changes in humidity during inhalation and exhalation. The study aimed to create a respiratory monitoring sensor entirely composed of plastic optical fibers. The sensor was designed with input and output POFs housed in 3D-printed sections connected by a flexible part, allowing for movement and attachment near the lung and diaphragm. This compact and portable sensor accurately captured human respiration signals and detected various breathing patterns. Comparisons with a commercial device for individuals in sitting and lying positions showed satisfactory agreement, with respiration rate measurements from the POF sensor and the commercial sensor differing by up to 4%. The all-plastic construction of the sensor enables its use in potentially electromagnetic hazardous environments like MRI scans[15].

2.3.6 “Parallel Polished Plastic Optical Fiber-Based SPR Sensor for Simultaneous Measurement of RI and Temperature” by Lian Liu, Jie Zheng, Shijie Deng, Libo Yuan and Chuanxin Teng (2021).

This research describes a parallel polished plastic optical fibre (POF) sensor based on surface plasmon resonance (SPR) for measuring refractive index (RI) and temperature at the same time. The sensor is made by symmetrically twice polishing the POF and coating both polished regions with gold. The inclusion of a polydimethylsiloxane (PDMS) layer on one side results in an extra temperature-sensing resonance peak in the transmission spectrum. The wavelength shifts of the two resonance peaks fluctuate with RI and temperature, allowing for simultaneous monitoring by measuring the shifts. The sensor has a high RI sensitivity of 1174 nm/RIU in the 1.335-1.37 range and a temperature sensitivity of 0.7 nm/°C in the 30°C-80°C range. Importantly, the results indicate no interference between the two sensing channels of the proposed sensor. The parallel polished structure offers advantages for developing multiparameter sensors with applications in biochemical sensing[16].

2.3.7 "U-Shaped Plastic Fiber Optic Sensor for Measuring Adulteration in Liquids via RGB Color Changes," by J. D. Filoteo-Razo et al.

Plastic fiber optic sensors have emerged as versatile tools for various sensing applications due to their flexibility, cost-effectiveness, and ease of fabrication. This literature review focuses on the article titled "U-Shaped Plastic Fiber Optic Sensor for Measuring Adulteration in Liquids via RGB Color Changes" by J. D. Filoteo-Razo et al., published in IEEE Sensors Letters. The review aims to provide insights into the research conducted by

the authors, highlighting the development and applications of the U-shaped plastic fiber optic sensor for liquid adulteration detection.

The article presents a novel approach using a U-shaped plastic fiber optic sensor to detect adulteration in liquids based on RGB color changes. Filoteo-Razo et al. offer a detailed analysis of the sensor's design, working principle, experimental setup, and performance evaluation. The literature review establishes the theoretical foundation by discussing relevant concepts and technologies related to fiber optic sensors and liquid adulteration detection. It emphasizes the significance of detecting adulteration in various liquids, such as food, beverages, and pharmaceuticals, and the challenges associated with conventional methods. The authors propose a U-shaped plastic fiber optic sensor as an effective solution, leveraging the principle of light transmission and RGB color sensing. Filoteo-Razo et al. present the experimental setup used to evaluate the performance of the U-shaped plastic fiber optic sensor for liquid adulteration detection. They outline the selection of materials, light sources, photodetectors, and signal processing techniques employed for accurate measurement of RGB color changes. The authors discuss the calibration process and the measurement procedures conducted to assess the sensor's sensitivity, selectivity, and response time. The results demonstrate the sensor's capability to detect and quantify different types of liquid adulterants[17].

2.3.8 “Humidity and Isopropyl Alcohol Detection Sensor Based on Plastic Optical Fiber” by Lorant A. Szolga (2021).

Attenuated This article looked at the abilities of plastic optical fiber for humidity monitoring and isopropyl alcohol as a high-risk flammable chemical. Many different businesses that need high levels of sensitivity and precision have found success with optical fiber sensors. In flammable materials where electricity poses a serious risk, electronic sensors are not allowed. In these conditions, optical fiber-based sensors are more than

welcome. Glass optical fibers have already demonstrated their great accuracy in measuring range of variables, from mechanical (elongation, pressure) to environmental (temperature, humidity), aspects. The interrogator's high price and the need for specialized personnel to install and maintain these glass fiber sensors are drawbacks. In some cases, a simple, inexpensive system that operates with excellent accuracy and sensitivity is a viable answer. This study was able to illustrate how the plastic optical fiber functions in comparison to an electronic humidity sensor by setting up a suitable testing environment. It also demonstrated how sensitive to isopropyl alcohol vapors an optical fiber-based sensors. If specific requirements were met, such as the use of an infrared LED and photodetector for transmitting and receiving light over the fiber, good connection and alignment of the fiber by polishing out the cladding, and at least 2 cm of the fiber's core exposed to the surrounding medium, this journal study showed the sensitivity of a plastic optical fiber as a humidity sensor[18].

2.3.9 “Fiber optic sensors based on circular and elliptical polymer optical fiber for measuring refractive index of liquids” by Fei Ye, Cui Tian, Cuihua Ma, Zhi Feng Zhang

Fiber optic sensors have emerged as powerful tools for various sensing applications due to their unique properties, such as high sensitivity, immunity to electromagnetic interference, and remote sensing capabilities. This literature review focuses on the article titled "Fiber Optic Sensors Based on Circular and Elliptical Polymer Optical Fiber for Measuring Refractive Index of Liquids" by Ye et al., published in Optical Fiber Technology. The review aims to provide insights into the research conducted by the authors, highlighting the development and applications of fiber optic sensors based on circular and elliptical polymer optical fiber for refractive index measurement of liquids. Fiber optic sensors have emerged as powerful tools for various sensing applications due to their unique properties, such as high sensitivity, immunity to electromagnetic interference, and remote sensing

capabilities. This literature review focuses on the article titled "Fiber Optic Sensors Based on Circular and Elliptical Polymer Optical Fiber for Measuring Refractive Index of Liquids" by Ye et al., published in Optical Fiber Technology. The review aims to provide insights into the research conducted by the authors, highlighting the development and applications of fiber optic sensors based on circular and elliptical polymer optical fiber for refractive index measurement of liquids.

The literature review establishes the theoretical foundation by discussing relevant concepts and technologies related to refractive index sensing and fiber optic sensors. It emphasizes the importance of refractive index measurement in various liquid-based applications, such as chemical analysis, biomedical diagnostics, and environmental monitoring. The authors propose the use of circular and elliptical POF sensors as practical solutions for refractive index sensing, exploiting the principles of light propagation and total internal reflection[19].

2.3.10 “Intensity-Modulated Polymer Optical Fiber-Based Refractive Index Sensor”
by Chuanxin Teng , Rui Min , Jie Zheng , Shijie Deng , Maosen Li , Li Hou and Libo Yuan.

In recent years, polymer optical fibers (POFs) have gained significant attention in the field of optical sensing due to their unique properties, including flexibility, cost-effectiveness, and ease of fabrication. This literature review focuses on the article titled "Intensity-Modulated Polymer Optical Fiber-Based Refractive Index Sensor: A Review" by Teng et al., published in Sensors. The review aims to provide insights into the research conducted by the authors, highlighting the development and applications of intensity-modulated POF-based refractive index sensors. The literature review establishes the theoretical foundation by discussing relevant concepts and principles related to refractive index sensing and POFs. It emphasizes the importance of refractive index measurement in

various applications, such as environmental monitoring, biomedical diagnostics, and chemical analysis. The authors propose the use of intensity modulation techniques in POF-based sensors to achieve accurate and reliable refractive index measurements.

The article describes the principles and configurations of intensity-modulated POF-based refractive index sensors. Teng et al. discuss different techniques used to modulate the intensity of light transmitted through the POF, such as bending, tapering, and coupling with other optical elements. They outline the design considerations and trade-offs involved in selecting the appropriate sensor configuration for specific applications. The article provides a comprehensive evaluation of the performance characteristics of intensity-modulated POF-based refractive index sensors. Teng et al. discuss key parameters such as sensitivity, linearity, dynamic range, and response time. They present experimental results and compare the performance of different sensor configurations and signal detection methods. The review emphasizes the potential of intensity-modulated POF-based sensors for achieving high sensitivity and reliable refractive index measurements. The article on "Intensity-Modulated Polymer Optical Fiber-Based Refractive Index Sensor: A Review" by Teng et al. provides a comprehensive overview of intensity-modulated POF-based refractive index sensors. The literature review offers insights into the principles, configurations, signal detection methods, and performance characteristics of these sensors. The authors' research contributes to the field of POF-based sensing by demonstrating the potential of intensity modulation techniques for accurate and reliable refractive index measurements. This literature review serves as a valuable resource for researchers interested in the development and application of intensity-modulated POF-based refractive index sensors[20].

2.4 Summary of literature

No of reference	Type of Optical Fiber	Sensing Application	Sensitivity	Wavelength	Year
[11]	Plastic Optical Fiber (POF)	Body temperature	30.071 mv/c	-	2020
[12]	Plastic Optical Fiber (POF)	Refractive index	1.33 to 1.41	620-750 nm	2022
[13]	Plastic Optical Fiber (POF)	Refractive index	1541%/RIU	-	2020
[14]	Plastic Optical Fiber (POF)	Refractive index, temperature	-0.596 nm/°C	680 nm / 800 nm	2022
[15]	Plastic Optical Fiber (POF)	Respiration monitoring	-	-	2017
[16]	Plastic Optical Fiber (POF)	Refractive index, temperature	1174 nm/RIU	360 nm– 2500 nm	2021
[17]	Plastic Optical Fiber (POF)	Adulteration detection in liquids	154 dB/RIU	50–1000 nm	2021
[18]	Plastic Optical Fiber (POF)	Humidity	-	940 nm	2021
[19]	Polymer Optical Fiber (POF)	Refractive index of liquids	- 66.58 dB/RIU	-	2021
[20]	Polymer Optical Fiber (POF)	Refractive index.	0.0024 mV	532, 633 and 780 nm	2021

2.5 Hardware Implementation

2.5.1 Light Emitting Diode (LED)

LEDs represent a solid-state lighting technology capable of providing intense illumination when appropriately configured in luminaires. Widely recognized as the most energy-efficient light source, the effectiveness of LEDs is contingent upon the wavelength of the emitted light. Red and blue wavelengths are commonly acknowledged as more efficient than green or orange wavelengths, contributing to the higher efficiency of luminaires employing materials in these colors. It is noteworthy that ongoing technical advancements, especially in LED lighting, are accelerating, promising even more efficient LEDs compared to alternative lighting sources.



Figure 2.7 Light Emitting Diode (LED).

2.5.2 Phototransistors

The phototransistor serves as a semiconductor device with the capability to sense light levels and regulate the current between the emitter and collector according to the received light intensity. Its application extends to light detection, and its heightened sensitivity, owing to the gain provided by its bipolar transistor nature, makes it more effective than other light-sensing devices. Consequently, phototransistors find optimal suitability in various applications.



Figure 2.8 Phototransistors.

2.5.3 Digital Humidity Temperature Meter

The Digital Humidity Temperature Meter, UT-333S, is known for its precision, stability, and safety. Its split-type design facilitates swift and accurate temperature detection across diverse environments. Particularly advantageous for monitoring challenging spaces such as small ventilation ducts, the handheld temperature and humidity meter's split-type construction proves beneficial. The UT-333S digital humidity temperature meter is shown in Figure 2.9.



Figure 2.9 Digital Humidity Temperature Meter

2.5.4 Amplifier Circuit

The amplifier circuit comprises resistors, IC sockets, capacitors, and includes a female header connector for elements like the NodeMCU, LED, LCD, phototransistor, and variable resistor, as depicted in Figure 2.10.



Figure 2.10 Amplifier circuit.

2.5.5 Plastic Optical Fiber Sensor

Measuring external forces using plastic optical fibers can be achieved through three distinct methods: intensity modulation, phase modulation, and Bragg wavelength shift. These techniques serve as the basis for developing specialized POF varieties tailored for precise and accurate sensor applications. Beyond its cost-effectiveness, POF stands out as a sensor material due to its chemical resistance and inert properties, ensuring fundamental safety. The optical fiber's mechanical protection is provided by the jacket or coating, enhancing its robustness. Typically constructed from polyethylene, alternative materials like polyvinylchloride and chlorinated polyethylene are also suitable. The core, surrounded by cladding with a lower refractive index, facilitates the propagation of light, ensuring efficient transmission.

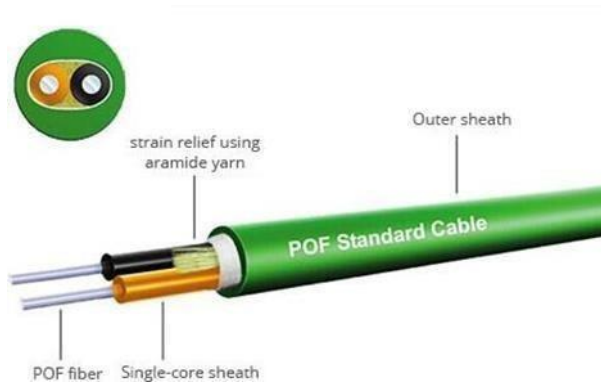


Figure 2.11 Plastic Optical Fiber Sensor.

2.5.6 NodeMCU

The NodeMCU, short for Node Microcontroller Unit is a development environment that encompasses both open-source software and hardware. It is built upon the ESP8266, a cost-effective System-on-a-Chip. NodeMCU is compatible with various development environments, including the Arduino IDE (Integrated Development Environment). The addition of Arduino support was developed by the NodeMCU/ESP8266 community, demonstrating an enhanced level of IDE integration. The component diagram in Figure 2.12 illustrates the NodeMCU.

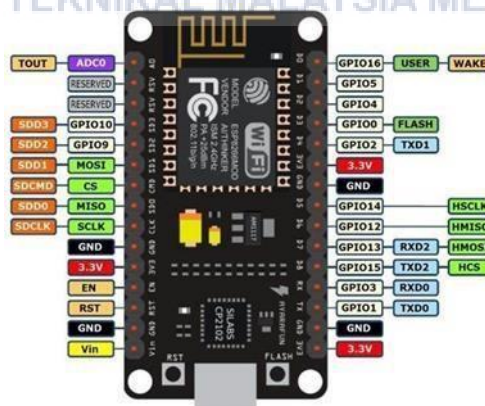


Figure 2.12 NodeMCU.

2.6 Summary

A more thorough comprehension of plastic optical fiber may now be possible thanks to the extensive literature evaluations mentioned above. Numerous authors from a wide range of disciplines base their development and design on their original and fascinating advice. A proper and complex project has been explored because of the numerous literature reviews mentioned above, and an objective can be successfully attained. The development of the U-shaped tapered plastic optical fiber sensor for humidity applications would receive several improvements. There are additional developments and project recommendations in the forthcoming chapter.



CHAPTER 3

METHODOLOGY

3.1 Introduction

The methodology provides a thorough review of a wide range of research paradigms and methods, as well as the tools and techniques that support them. The purpose of this chapter is to concentrate on the general research and hardware process flow, as well as the design approach. This methodology's organized strategy includes conducting research through journals and articles, designing a project's design, and required elements, installing hardware into the project, testing the project, resolving difficulties that develop, and creating a report. Any project necessitates an organization that elaborates on the method for completion. To do that, a detailed flow chart demonstrating the processes required to complete the project from start to finish is prepared. Aside from that, it is essential to understand the hardware tool that will be used before beginning this project.

3.2 Methodology

The purpose of project methodology is to assure the success of specific processes, approaches, techniques, methodologies, and technologies throughout the management process by enabling effective decision-making and problem-solving.

3.2.1 Flowchart

The figure 3.1 shows the flowchart of project implementation. The flowchart below represents the project's overall workflow.

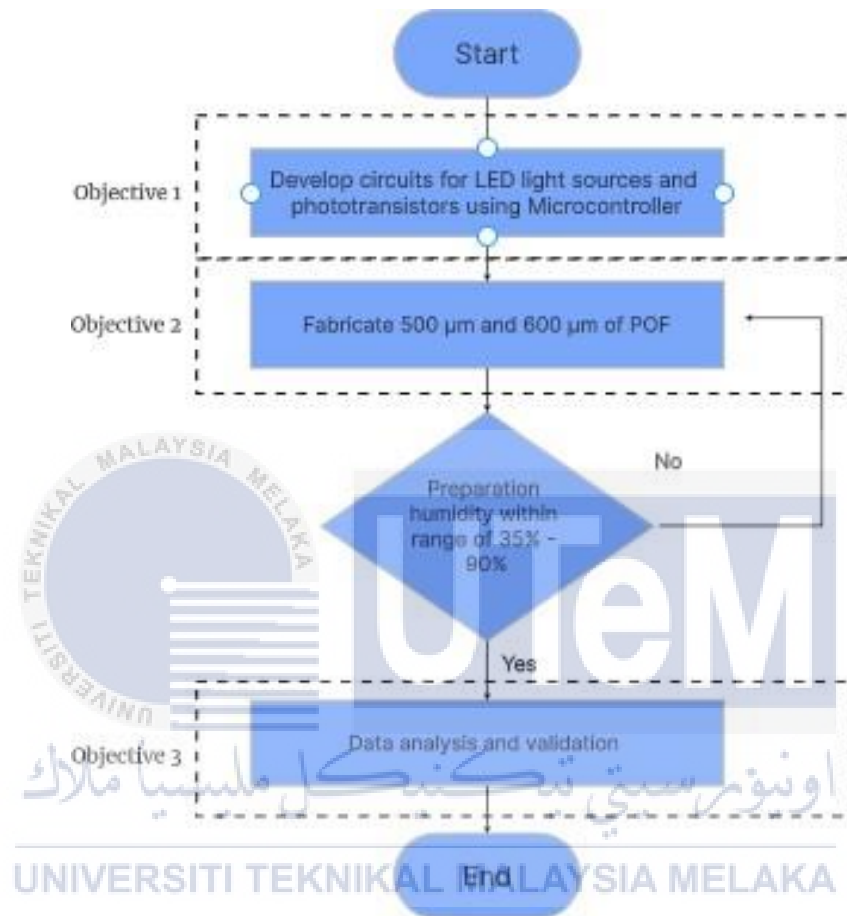


Figure 3.1 Flowchart of the project

3.2.2 Fabrication of Tapered Plastic Optical Fiber (POF)

Figure 3.2 shows the plastic optical fiber (POF) model SH4001 Super Eska with 980um core and 1000um cladding diameter respectively.



Figure 3.2 Plastic Optical Fiber

Figure 3.3 shows the preparation of fiber optic and wire strippers, a POF cutter, and a ruler. These pieces of equipment are used to measure and cut plastic optical fiber (POF) cables. A folding knife, sandpaper, micrometer, and markers are also required for this technique.



a) Stripper



b) POF cutter

Figure 3.3 Fiber optic and wire stripper, POF cutter and ruler.

With a pen or something visible, measure and mark the length of the 20cm cable POF. Then, by using a fiber optic and a wire stripper, cut the length of the POF to 20 cm as needed. Using pens, markers, or other objects which can mark to be seen to cut, measure and mark at the POF cable's midpoint for up to 3 cm in length. After that, by using a POF cutter, cut the 3 cm mark at the POF cable's midpoint. In addition to that, the POF cable jacket removed using a folding knife. Figure 3.4 shows the results after the jacket is removed.

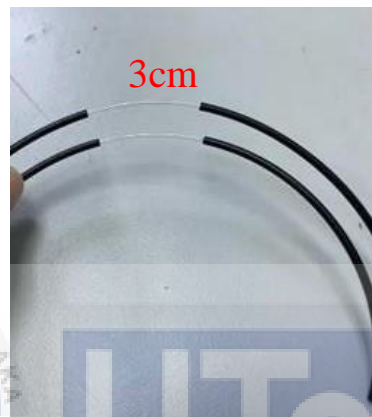


Figure 3.4 POF cable after the middle is cut.

Then, the tapered POF was followed by polishing the core fiber using sandpaper of 1000 grit. Thin the POF cable (core) in the middle on both sides (double side) using sandpaper and measure with a micrometer until the appropriate size is achieved. The layer condition of a tapered POF cable after polishing the core fiber is shown in the illustration. Limitation of proposed methodology.

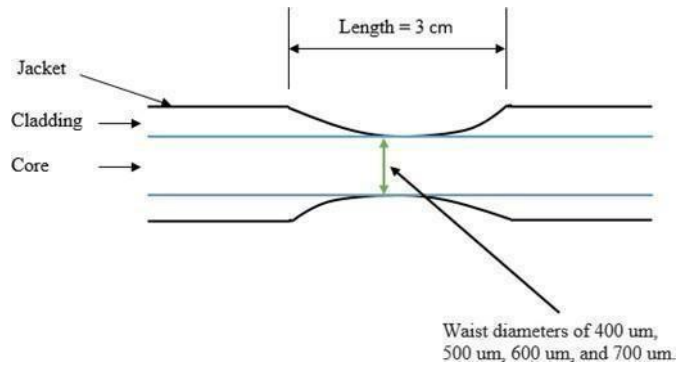


Figure 3.5 POE cable after the middle is cut.

A digital micrometer is regularly used to measure the stripped area to guarantee that the aimed tapered fiber waist diameter value is specific. After polishing the core fiber, take measurements using a digital micrometer as shown in Figure 3.7.



Figure 3.6 Thickness of POE cable.



Figure 3.7 Digital micrometer

Figure 3.8 shows how it is measured. Using 1000 grit sandpaper, polish the core fiber. Digital micrometers were used on a regular basis to measure the stripped area to ensure that the tapered fiber's waist diameter was 500 μm and 600 μm as in Figure 3.9 (a) and (b).



Figure 3.8 shows the measurement of stripped area.

3.3 Experimental Setup

The experimental setup for POF sensing in this project is shown in Figure 3.18 (f). Start the setup for this project. It consists of a LED light, a chamber, digital temperature humidity, a phototransistor, an amplifier circuit and a battery. Figure 3.9 display the preparation of LED light and phototransistor.

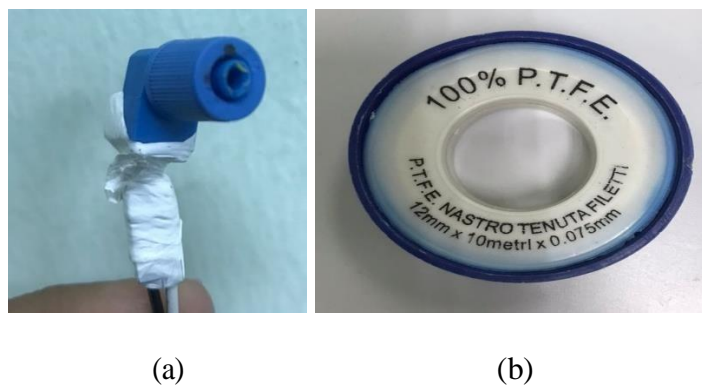


Figure 3.9 Shows the LED light (a) and tape (b).

Attach the phototransistor and LED light to the jumper as in Figure 3.9 (a) using tape as in Figure 3.9 (b). Then, construct the project's chamber. Measure the size of each component and mark it. Use masking tape, stick, mark, and iron solder to make holes. Figure 3.10 displays the process of constructing a chamber.



Figure 3.10 Solder the container to make the hole.

Try out the hollowed-out space using real components. Figure 3.11 show currently adjusting the item's component with the hole that has been made. After finishing the adjustment, wrap the chamber with black tape and then insert the component to be placed in the chamber into the hole that has been made, as in Figure 3.11. Black tape was used to completely cover the chamber, preventing outside light from penetrating.

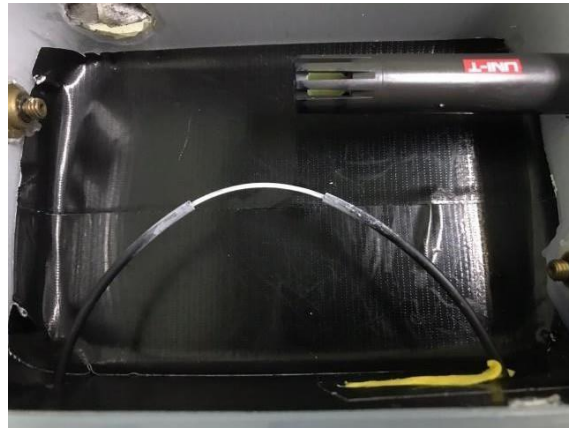


Figure 3.11 Adjusting the item's component and chamber covered with black tape.

The components of the experimental setup and the experimental setup for humidity sensing are shown in Figure 3.12.



(a)



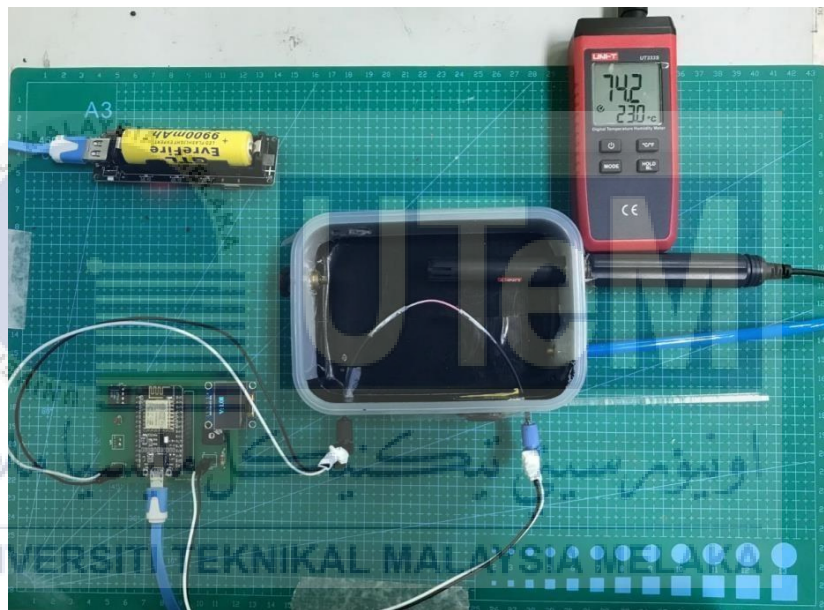
(b)



(c)



(d)



(e)



(f)

Figure 3.12 Shows the hardware components: (a) amplifier circuit, (b) digital humidity temperature, (c) battery, (d) LED light and phototransistor, (e) Component arrangement, and (f) Experimental setup.

Referring to Figure 3.12, the battery was employed to power the amplifier circuit, LED, and phototransistor. Simultaneously, the LCD connected to the amplifier circuit served to monitor the humidity sensing output voltage. For the detection of relative humidity, one end of the sensor linked to the LED light, while the other end connected to the phototransistor. The impact of optical fibers on light transmission was extensively investigated using red LED (645 nm), green LED (530 nm), and blue LED (470 nm) wavelengths. The optical fiber's transformation of light into an electrical signal was achieved through a phototransistor. To ensure sensor reliability, the experiment was conducted three times for each 5% relative humidity level, starting from 35% relative humidity.

3.4 Summary

In summary, this chapter presents a detailed account of the methodology employed in developing the humidity sensor as representative to refractive index sensor. It covers the experimental setup, fiber fabrication, measurement procedure, and calibration experiments. This chapter establishes the foundation for the subsequent analysis and interpretation of the collected data in the following chapters. To validate the accuracy of the sensor, the researchers conduct a series of calibration experiments using known liquid samples with different refractive indices. They compare the obtained results with theoretical calculations and demonstrate good agreement, thus confirming the reliability of their sensor design.



CHAPTER 4

RESULTS AND DISCUSSIONS

4.1 Introduction

The results and analysis of the Development of a Refractive Index Sensor Based on Changes in the Radius of a U-Shaped Plastic Optical Fibre are provided in this chapter. This chapter will go through the results of the tapered POF sensor's sensitivity with humidity. This chapter will consist of data analysis from the graph.

4.2 Results and Analysis

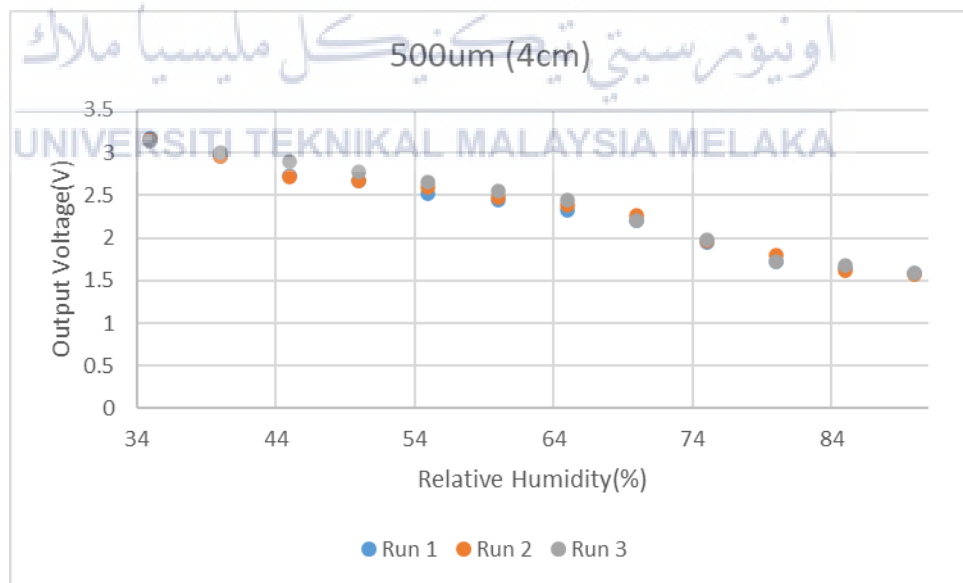
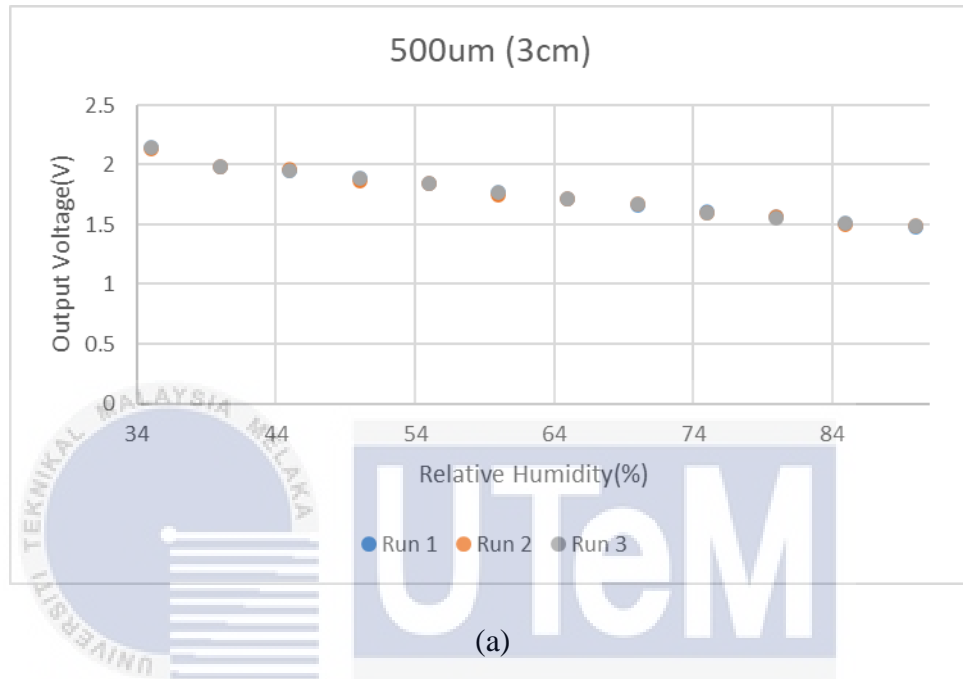
In this project, a total of two different waist-diameter tapered POFs were used. The waist diameters used were 500 μm and 600 μm for U-shaped tapered POF. This measurement was conducted three times between 35% RH and 90% RH. The output measurement was recorded in voltages (V) from LCD at amplifier circuit.

4.2.1 Repeatability Test

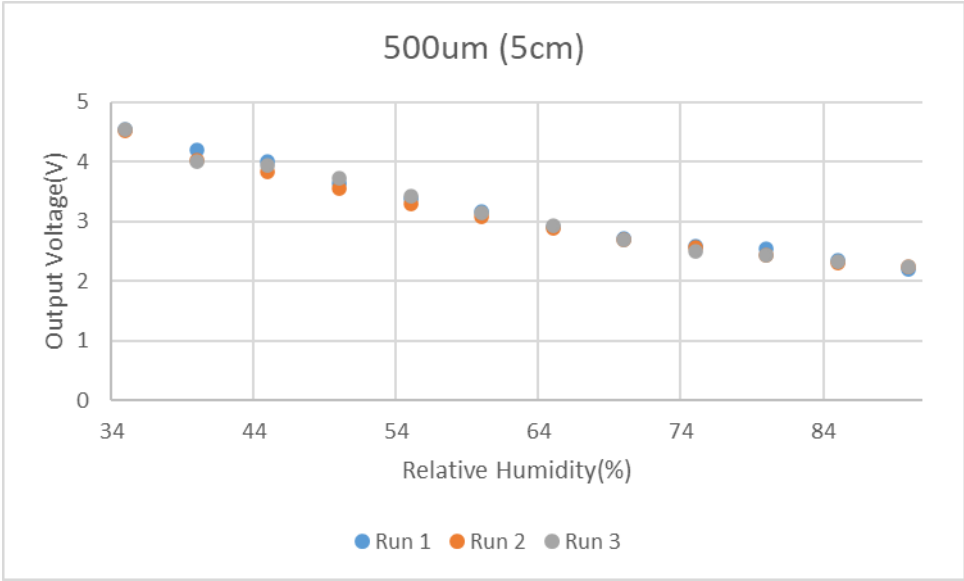
A repeatability test was done to see the consistency of repeated measurements. To evaluate the sensor performance, output voltage of humidity at wavelength of red (645 nm), green (530 nm) and blue (470 nm), were observed as shown in graph of Figure 4.1, Figure 4.2 and Figure 4.3.

4.2.1.1 Red (645 nm)

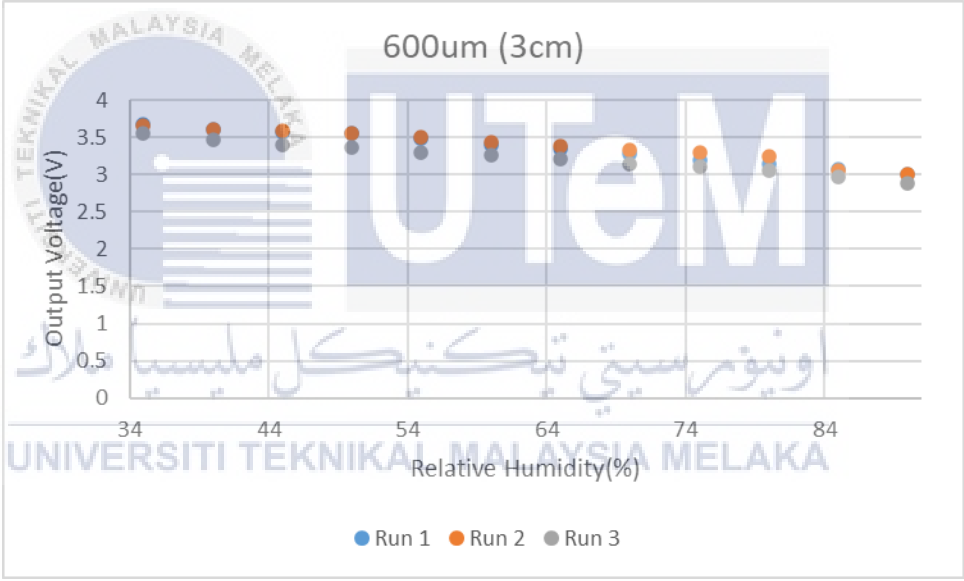
Begin by experimenting with the red wavelength for all types of waist diameter. The graph in Figure 4.1 depicts the repeatability test of the U-shaped tapered POF against humidity for the red wavelength.



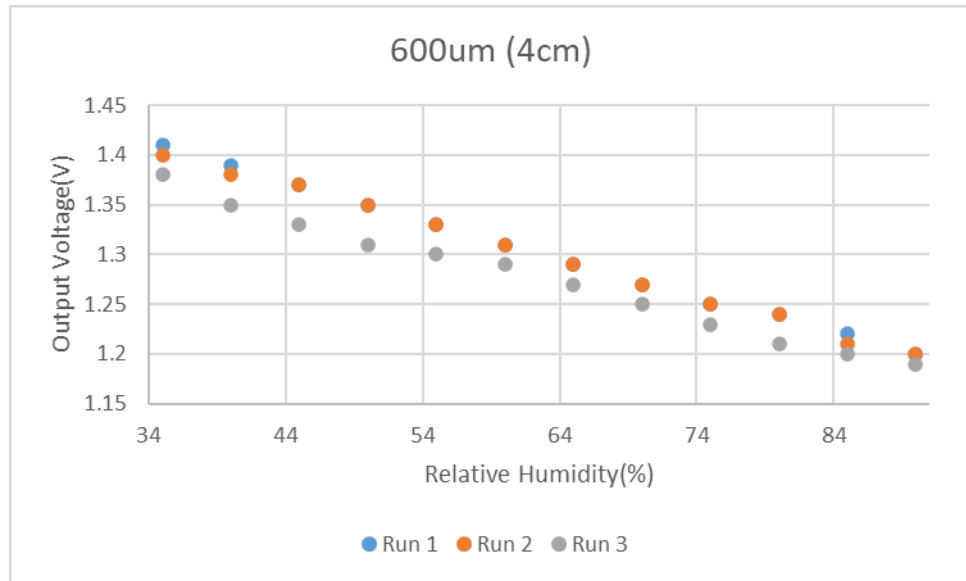
(b)



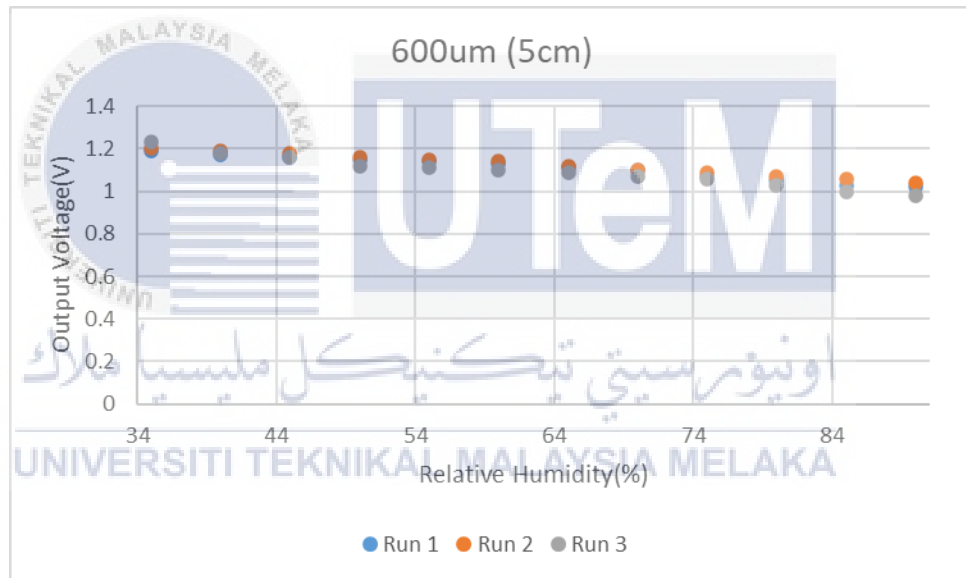
(c)



(d)



(e)



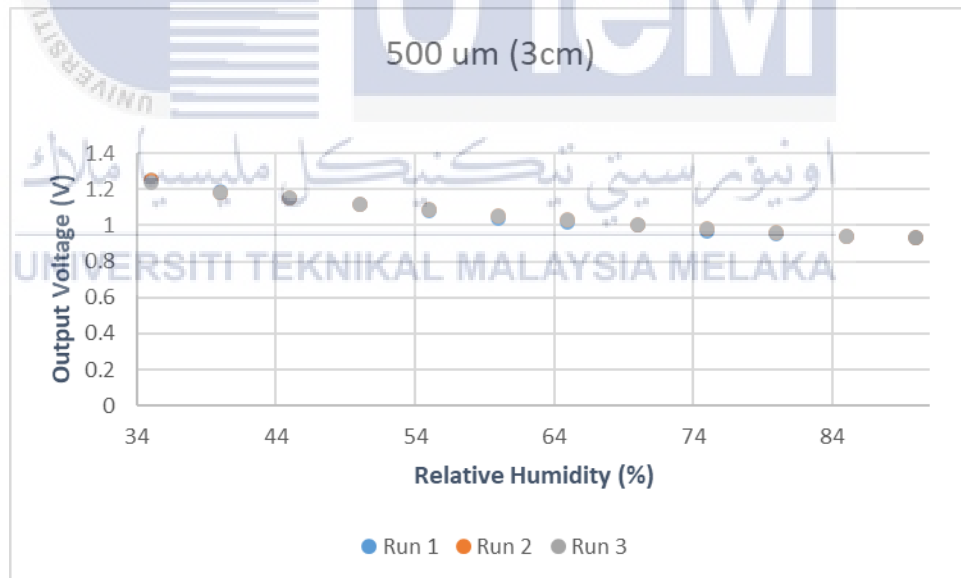
(f)

Figure 4.1 The repeatability test of (a) 500 μm (3cm), (b) 500 μm (4cm), (c) 500 μm (5cm) , (d) 600 μm (3cm), (e) 600 μm (4cm) and (f) 600 μm (5cm) for red wavelength.

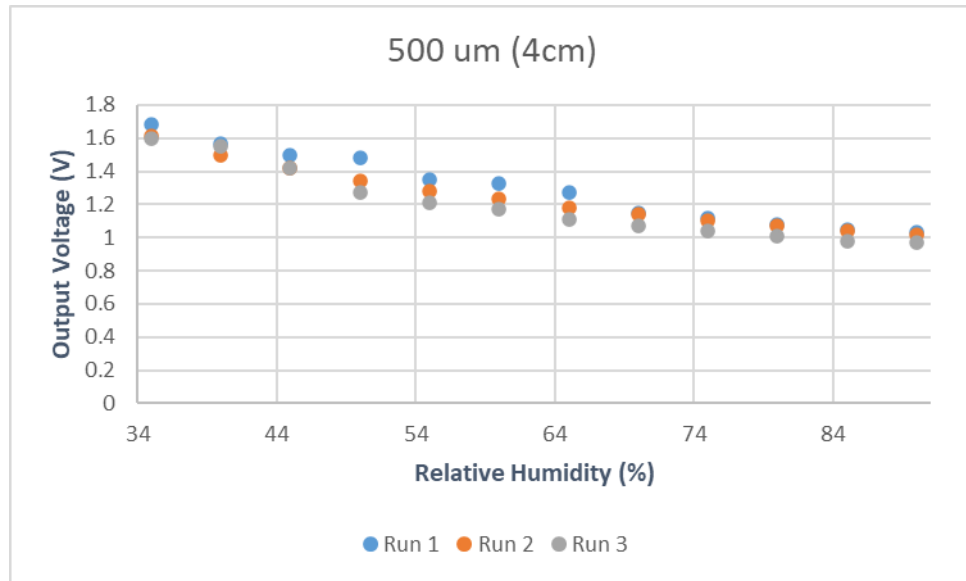
It is noticeable that with an increase in relative humidity from 35% to 90%, there is a corresponding decrease in the output voltage. Conversely, when the relative humidity ranges from 90% to 35%, the output voltage demonstrates an increase. The notable variations in output voltage between runs 1, 2, and 3 at each humidity level and for each waist diameter of the U-shaped tapered POF contribute to the observed irregular shifts. However, the output voltage consistency improves in instances where there is a smaller gap. Specifically, the U-shaped tapered POF with a waist diameter of 500 μm exhibits superior consistency in output voltage.

4.2.1.2 Green (530 nm)

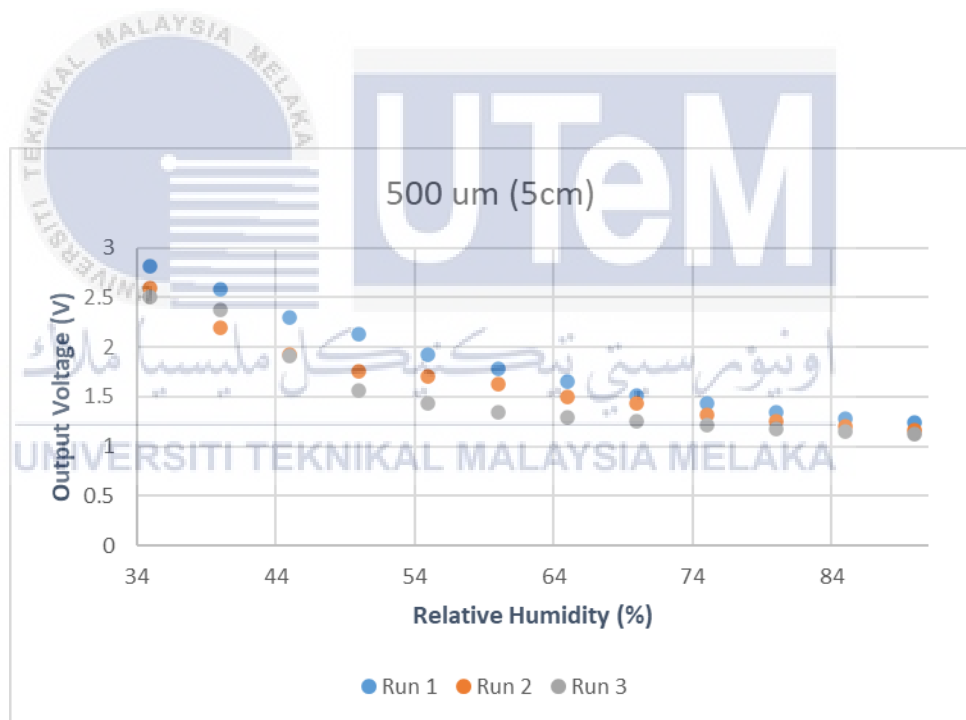
Figure 4.2 shows the graph for the repeatability test of the U-shaped tapered POF against humidity for the green wavelength.



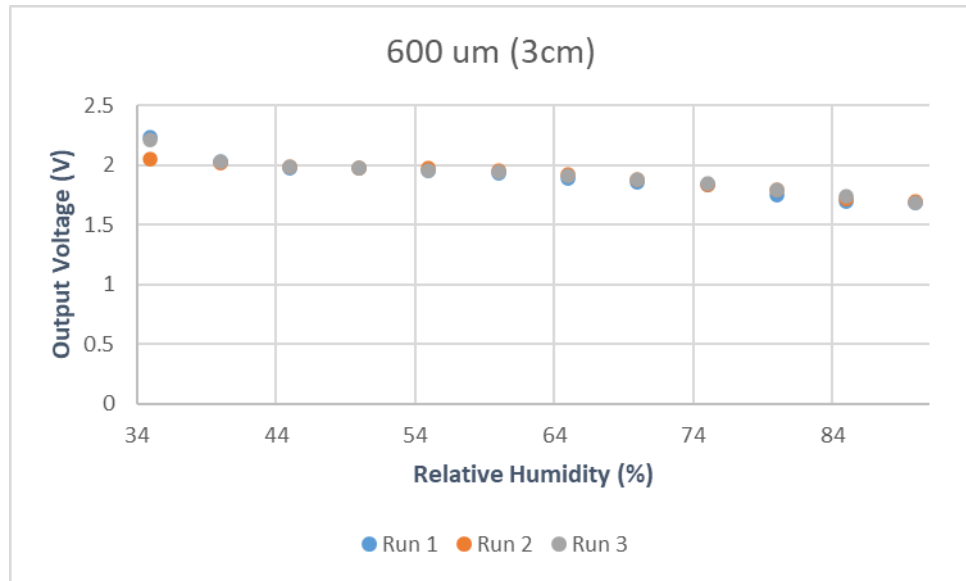
(a)



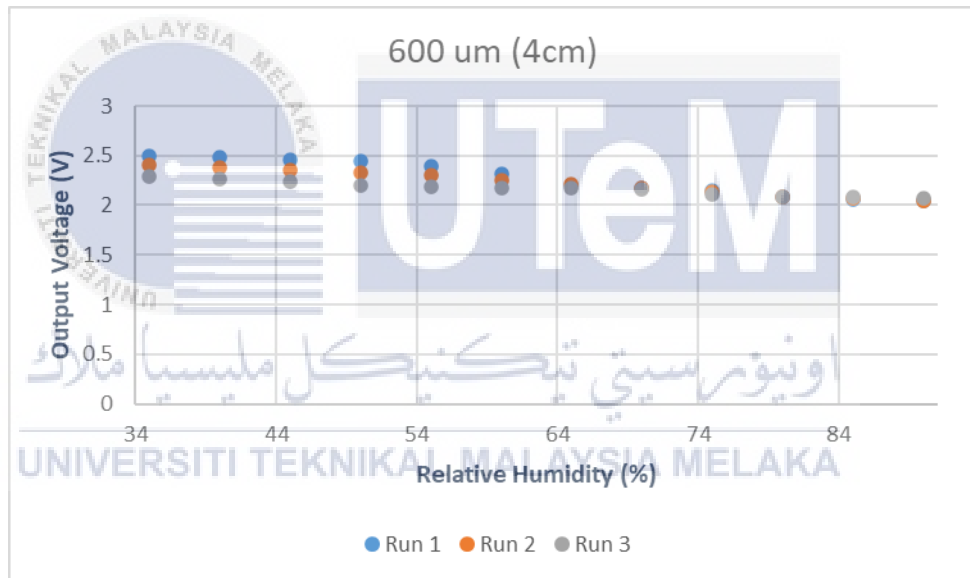
(b)



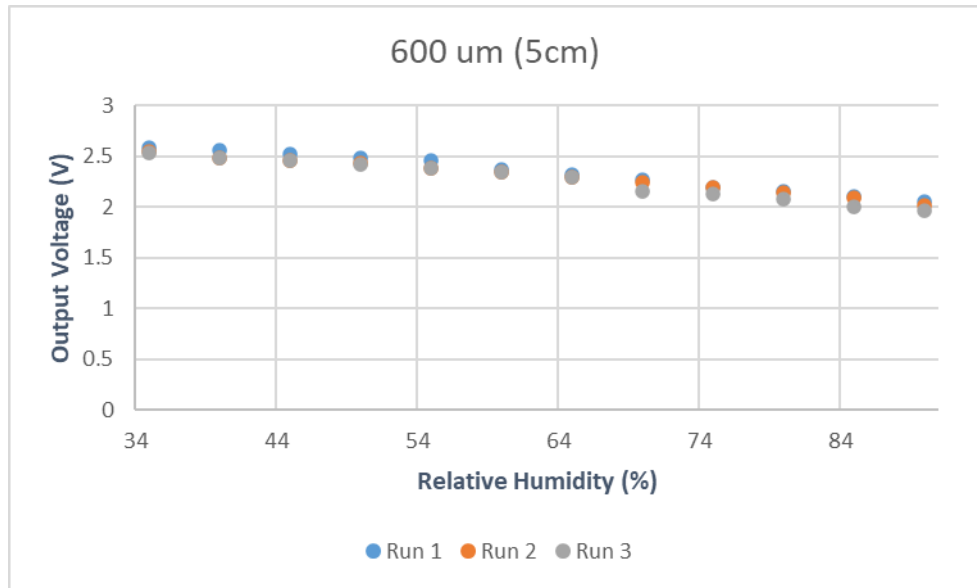
(c)



(d)



(e)



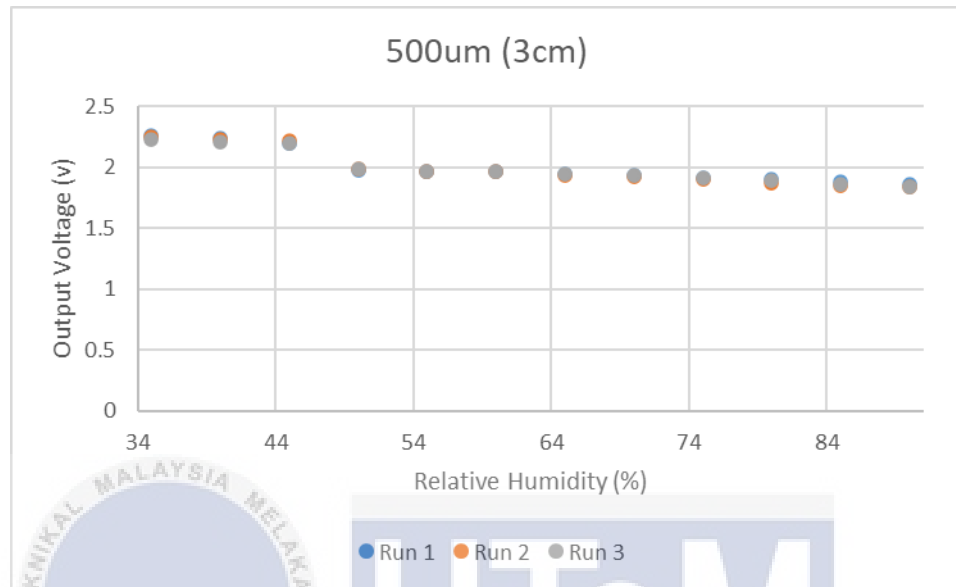
(f)

Figure 4.2 The repeatability test of (a) 500 μm (3cm), (b) 500 μm (4cm), (c) 500 μm (5cm), (d) 600 μm (3cm), (e) 600 μm (4cm) and (f) 600 μm (5cm) for green wavelength.

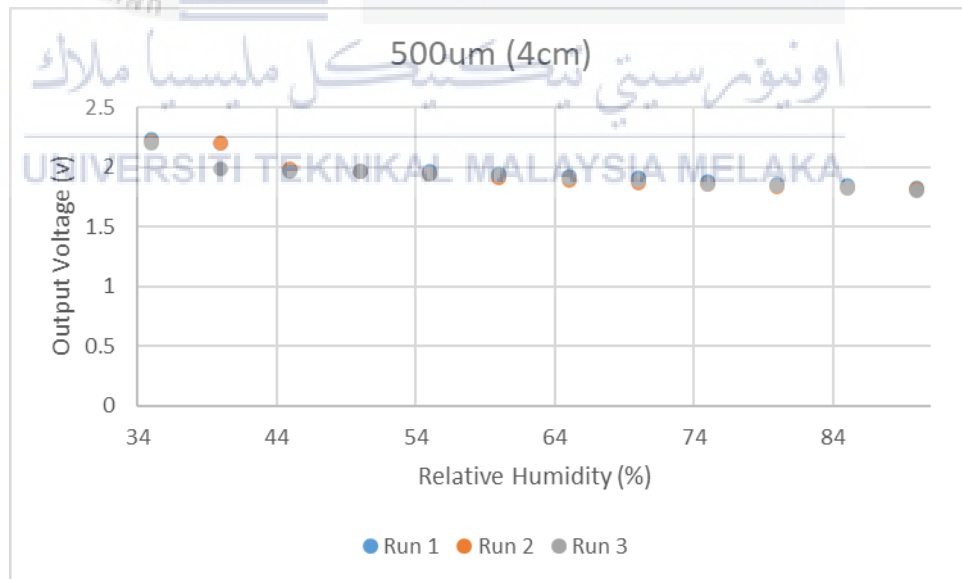
The data reveals a decrease in output voltage as relative humidity rises from 35% to 90%, followed by an increase as relative humidity decreases from 90% to 35%. Notably, the U-shaped tapered POF with a waist diameter of 500 μm exhibits less variability and showcases superior consistency in its output voltage.

4.2.1.3 Blue (470 nm)

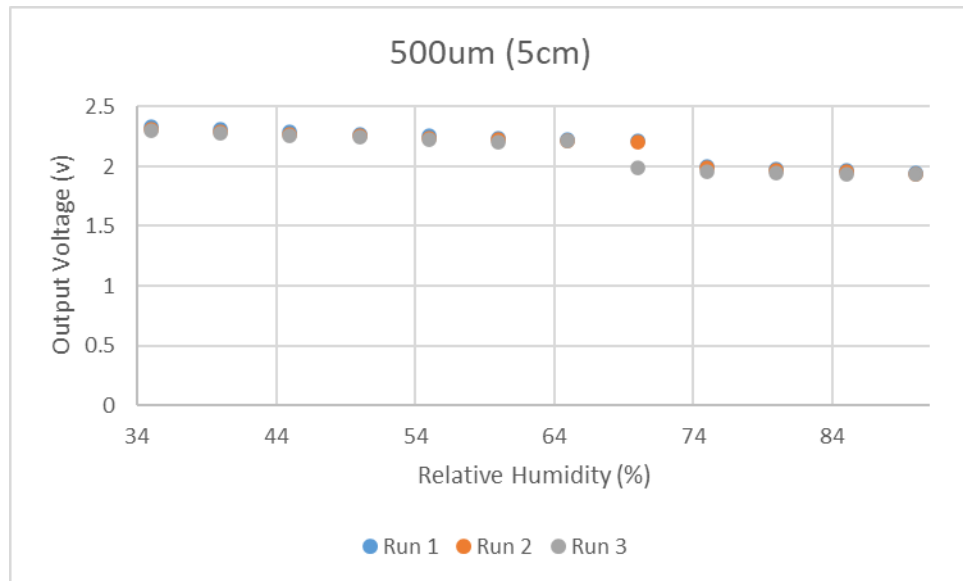
Figure 4.3 shows the graph for the repeatability test of the U-shaped tapered POF against humidity for the blue wavelength.



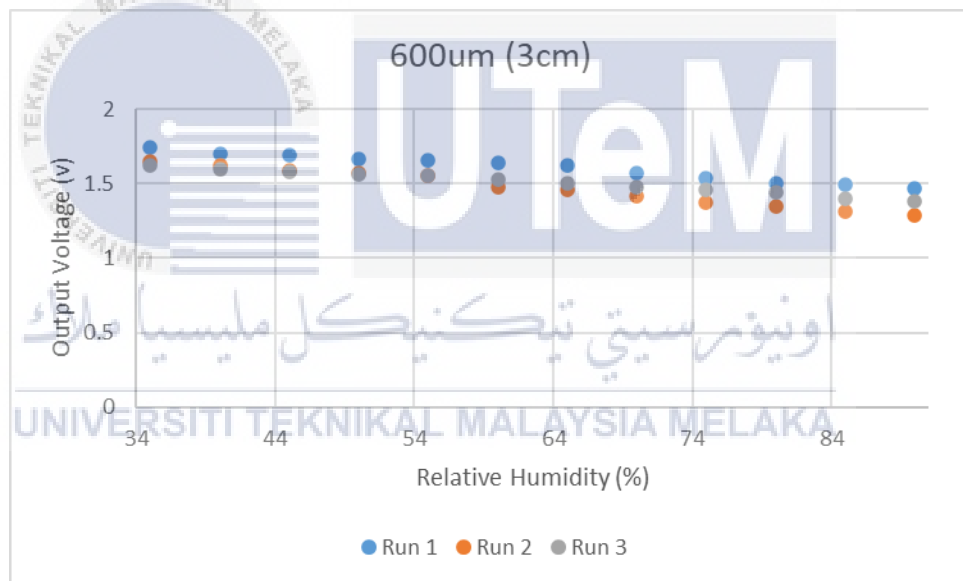
(a)



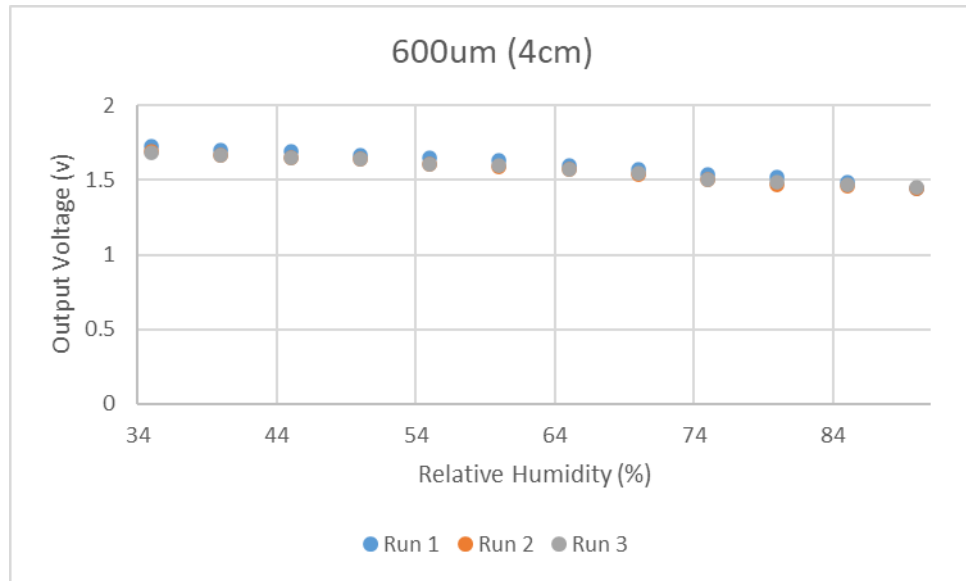
(b)



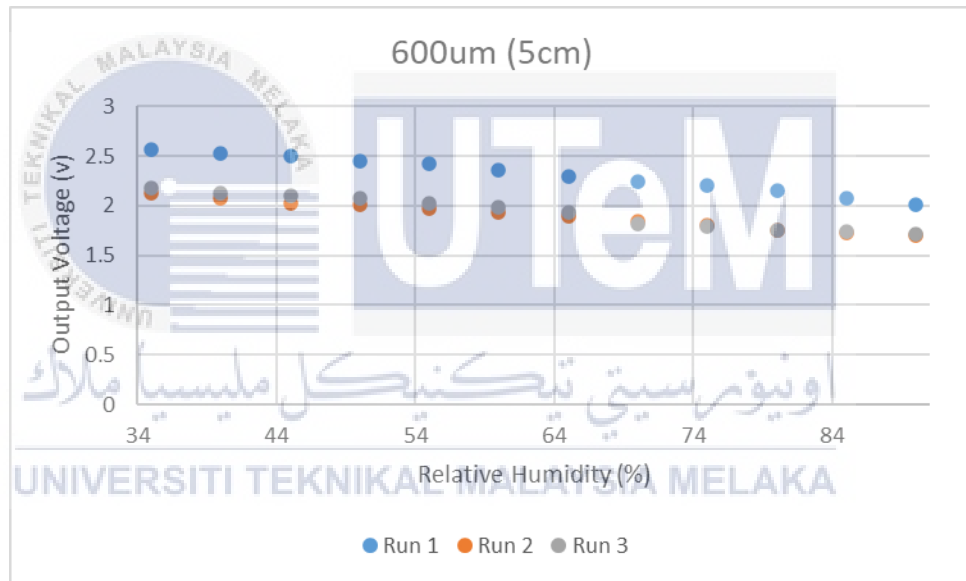
(c)



(d)



(e)



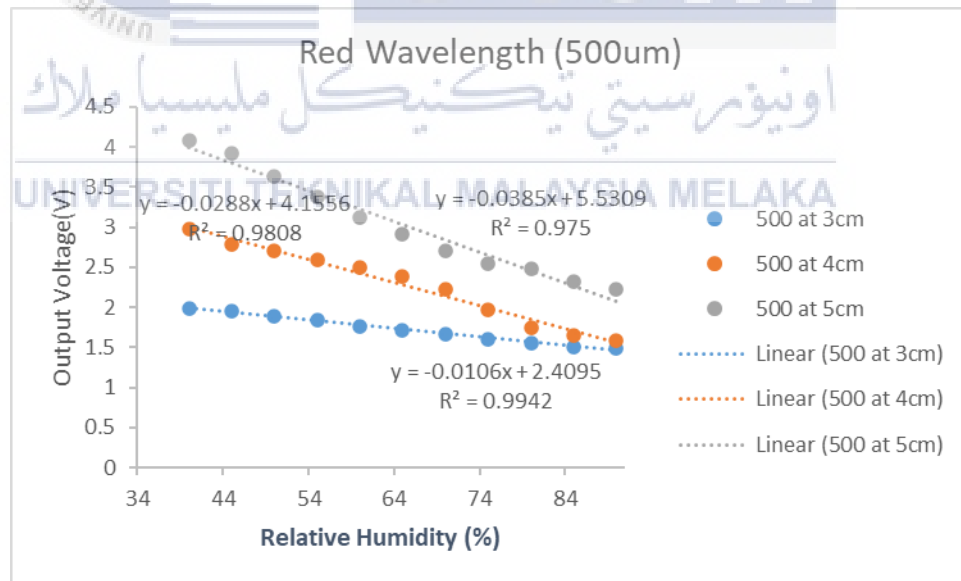
(f)

Figure 4.3 The repeatability test of (a) 500 μm (3cm), (b) 500 μm (4cm), (c) 500 μm (5cm) , (d) 600 μm (3cm), (e) 600 μm (4cm) and (f) 600 μm (5cm) for blue wavelength.

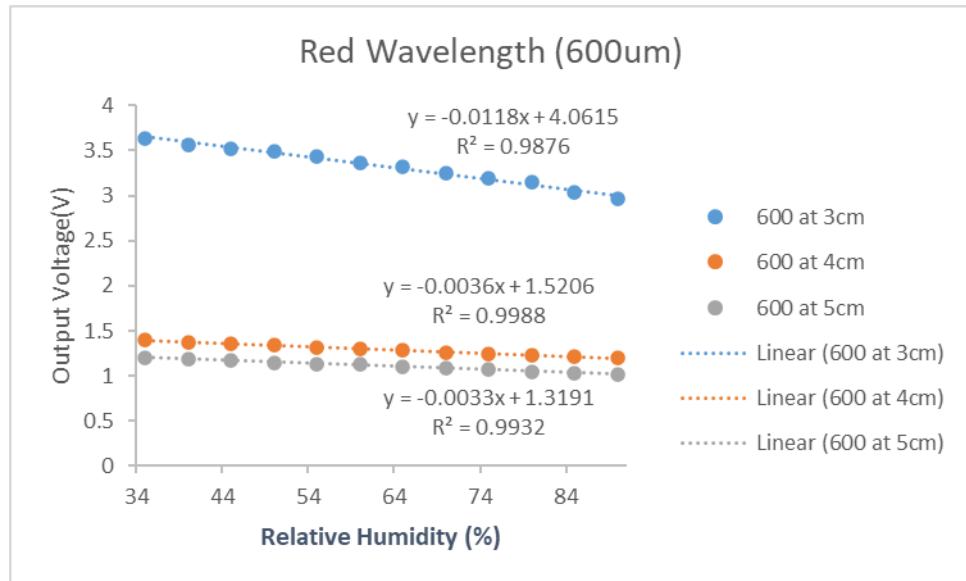
In all graphical representations, it is evident that the output voltage demonstrates an increase from 90% to 35% relative humidity, coupled with a decrease from 35% to 90% relative humidity. Notably, the U-shaped tapered POF with a waist diameter of 500 μm exhibits a narrower gap and enhanced stability in its output voltage. Across all light wavelengths, there is notable repeatability at the 500 μm waist diameter. These findings suggest that polished tapered POF absorbs more water particles, leading to increased fluctuations in the evanescent wave (EW) concerning the quantity of humidity adsorption necessary for optimal repeatability.

4.2.2 Trendline

Figure 4.3 shows the trendline of the U-shaped tapered POF against humidity for the red wavelength for waist diameter 500 μm and 600 μm at the radius of 3cm, 4cm, and 5cm.



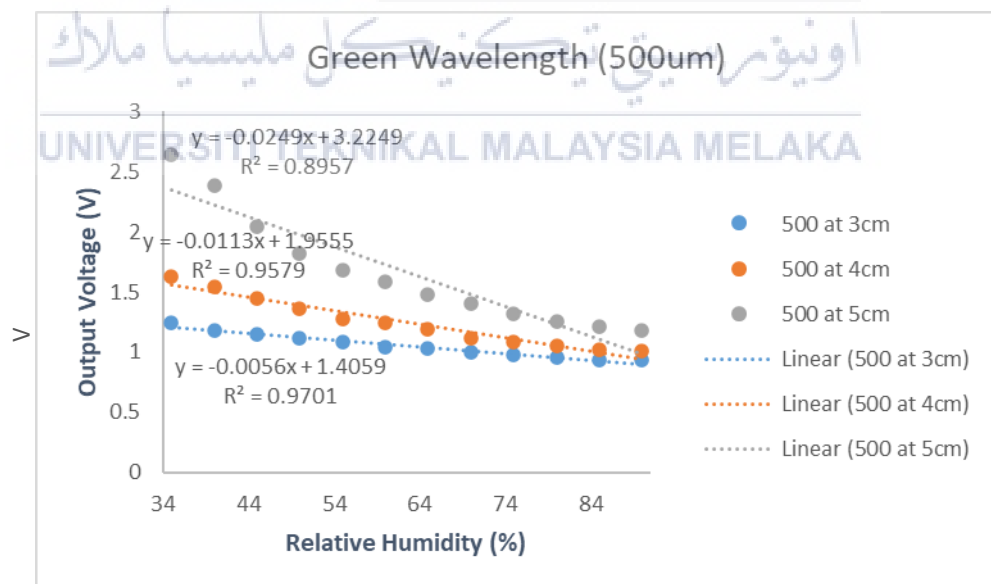
a)



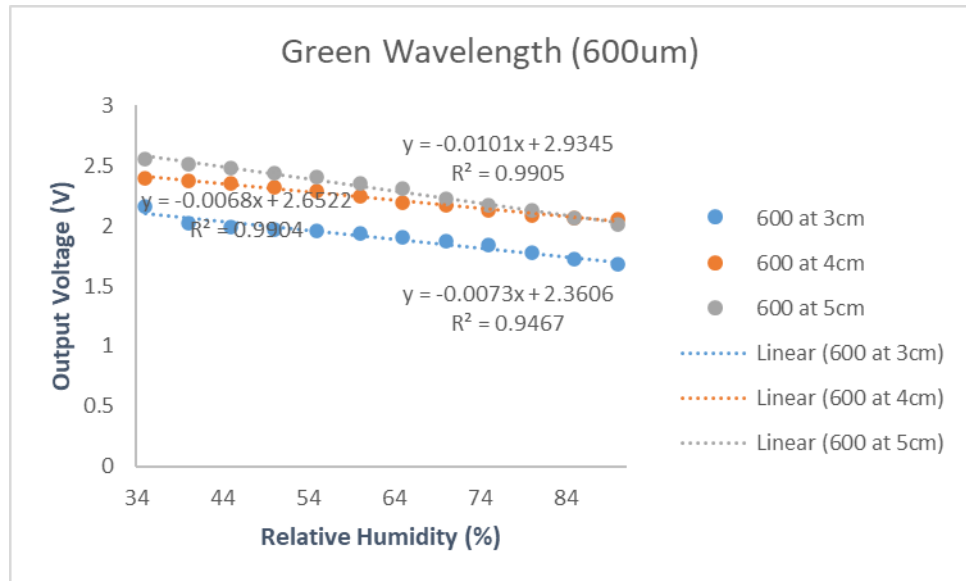
(b)

Figure 4.4 Trendline graph for the red wavelength.

Figure 4.5 shows the trendline of the U-shaped tapered POF against humidity for the green wavelength.



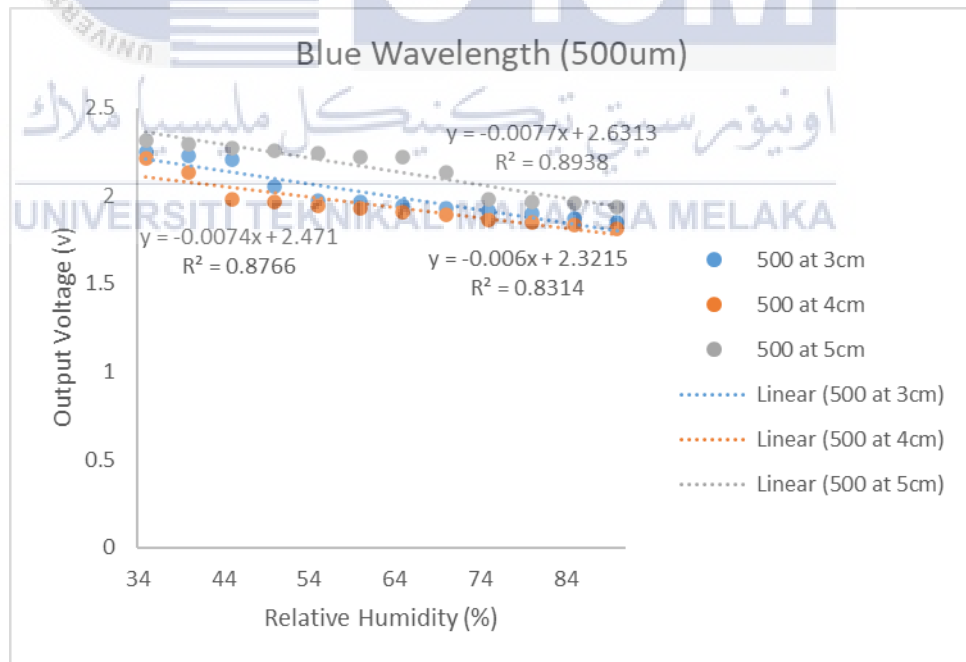
(a)



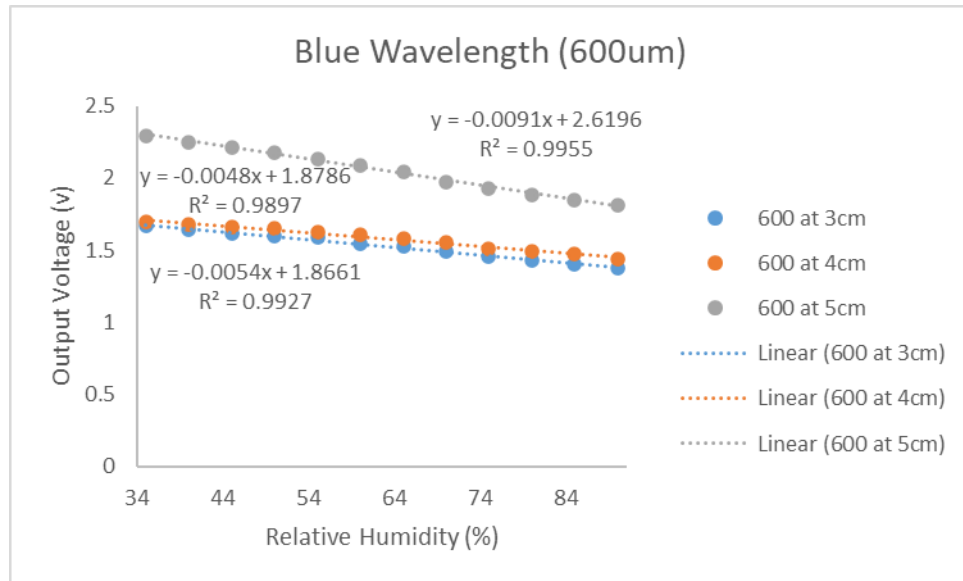
(b)

Figure 4.5 Trendline graph for the green wavelength.

Figure 4.6 shows the trendline of the U-shaped tapered POF against humidity for the blue wavelength.



(a)



(b)

Figure 4.6 Trendline graph for the blue wavelength.

As the RH levels increased, the output voltages for polished tapered POF's waist diameter fell linearly. The slope of the curve between output voltage and percent relative humidity serves as a measure of a sensor's sensitivity. The 500 μ m waist diameter has higher sensitivity and linearity than the other waist diameters for all wavelength.

Tables 4.1, 4.2, and 4.3 show a summary of the sensor performance for the four waist diameters of tapered POF, as well as the sensitivity, linearity, and resolution. All waist diameter U-shaped tapered POF sensors showed superiority in terms of sensing performance, with more than 95% linearity. The standard deviation is the amount of variation from the average value of repeated measurement data, whereas the resolution is the minimum relative humidity percentage of the specified sensor, which is calculated by dividing the standard deviation by the sensitivity.

Based on Table 4.1, the highest sensitivity was obtained with the 500 μm tapered POF, which was 0.0106 V/% with a minimum resolution of 0.53%. The lowest sensitivity was obtained with the 600 μm tapered POF, which was 0.0118V/% with a maximum resolution of 7.40%.

	Wavelength	
	Red = 645 nm (3cm)	
Waist Diameter (μm)	500 μm	600 μm
Sensitivity (V/%RH)	0.0106	0.0118
Linearity (%)	99.7095	99.3780
Resolution (%RH)	0.532508073	7.407272001

Table 4.1 The characteristics of a U-shaped

tapered POF for the red wavelength for 3cm.

Based on Table 4.2, the highest sensitivity was obtained with the 500 μm tapered POF, which was 0.0288V/% with a minimum resolution of 1.50%. The lowest sensitivity was obtained with the 600 μm tapered POF, which was 0.0036V/% with a maximum resolution of 4.14%.

	Wavelength	
	Red = 645 nm (4cm)	
Waist Diameter (μm)	500 μm	600 μm
Sensitivity (V/%RH)	0.0288	0.0036
Linearity (%)	99.0353	99.9399
Resolution (%RH)	1.508510294	4.140798014

Table 4.2 The characteristics of a U-shaped tapered POF for the red wavelength for 4cm.

Based on Table 4.3, the highest sensitivity was obtained with the 500 μm tapered POF, which was 0.0385V/% with a minimum resolution of 1.29%. The lowest sensitivity was obtained with the 600 μm tapered POF, which was 0.0033V/% with a maximum resolution of 5.88%.

	Wavelength	
	Red = 645 nm (5cm)	
Waist Diameter (μm)	500 μm	600 μm
Sensitivity (V/%RH)	0.0385	0.0033
Linearity (%)	98.7420	99.6594
Resolution (%RH)	1.299633373	5.889776836

Table 4.3 The characteristics of a U-shaped tapered POF for the red wavelength for 5cm.

Based on Table 4.4, the highest sensitivity was obtained with the 500 μm tapered POF, which was 0.0056V/% with a minimum resolution of 0.60%. The lowest sensitivity was obtained with the 600 μm tapered POF, which was 0.0073V/% with a maximum resolution of 2.49%.

	Wavelength	
	Green = 530 nm (3cm)	
Waist Diameter (μm)	500 μm	600 μm
Sensitivity (V/%RH)	0.0056	0.0073
Linearity (%)	98.4936	97.2985
Resolution (%RH)	0.60140653	2.499868089

Table 4.4 The characteristics of a U-shaped tapered POF for the green wavelength.

Based on Table 4.5, the highest sensitivity was obtained with the 500 μm tapered POF, which was 0.0113V/% with a minimum resolution of 4.84%. The lowest sensitivity was obtained with the 600 μm tapered POF, which was 0.0068V/% with a maximum resolution of 8.5%.

	Wavelength	
	Green = 530 nm (4cm)	
Waist Diameter (um)	500 μm	600 μm
Sensitivity (V/%RH)	0.0113	0.0068
Linearity (%)	97.8723	99.5188
Resolution (%RH)	4.844269766	8.520316757

Table 4.5 The characteristics of a U-shaped tapered POF for the green wavelength.

Based on Table 4.6, the highest sensitivity was obtained with the 500 μm tapered POF, which was 0.0249V/% with a minimum resolution of 6.5%. The lowest sensitivity was obtained with the 600 μm tapered POF, which was 0.0101V/% with a maximum resolution of 3.7%.

	Wavelength	
	Green = 530 nm (5cm)	
Waist Diameter (um)	500 μm	600 μm
Sensitivity (V/%RH)	0.0249	0.0101
Linearity (%)	94.6414	99.5238
Resolution (%RH)	6.53559923	3.715541604

Table 4.6 The characteristics of a U-shaped tapered POF for the green wavelength.

Based on Table 4.7, the highest sensitivity was obtained with the 500 μm tapered POF, which was 0.006V/% with a minimum resolution of 1.49%. The lowest sensitivity was obtained with the 600 μm tapered POF, which was 0.0054V/% with a maximum resolution of 13.60%.

	Wavelength	
	Blue = 470 nm (3cm)	
Waist Diameter (um)	500 μm	600 μm
Sensitivity (V/%RH)	0.006	0.0054
Linearity (%)	93.6269	99.6343
Resolution (%RH)	1.490125428	13.60639889

Table 4.7 Characteristics of a U-shaped tapered POF for the blue wavelength.

Based on Table 4.8, the highest sensitivity was obtained with the 500 μm tapered POF, which was 0.0074V/% with a minimum resolution of 2.95%. The lowest sensitivity was obtained with the 600 μm tapered POF, which was 0.0048V/% with a maximum resolution of 3.99%.

	Wavelength	
	Blue = 470 nm (4cm)	
Waist Diameter (um)	500 μm	600 μm
Sensitivity (V/%RH)	0.0074	0.0048
Linearity (%)	91.1811	99.4836
Resolution (%RH)	2.958998701	3.993191871

Table 4.8 Characteristics of a U-shaped tapered POF for the blue wavelength.

Based on Table 4.9, the highest sensitivity was obtained with the 500 μm tapered POF, which was 0.0077V/% with a minimum resolution of 3.11%. The lowest sensitivity was obtained with the 600 μm tapered POF, which was 0.0091V/% with a maximum resolution of 25.30%.

	Wavelength	
	Blue = 470 nm (5cm)	
Waist Diameter (um)	500 μm	600 μm
Sensitivity (V/%RH)	0.0077	0.0091
Linearity (%)	94.5409	99.7747463
Resolution (%RH)	3.111642874	25.30065969

Table 4.9 Characteristics of a U-shaped tapered POF for the blue wavelength.

The slope of the curve between the output voltage (V) and relative humidity (%) is used to describe the sensor's sensitivity. Based on Table 4.4, the highest sensitivity was obtained with the 500 μ m tapered POF of green wavelength, which was 0.0117 V/% with a minimum resolution of 0.61%. The green wavelength of 500 μ m has the highest sensitivity of 0.0117 V/%.

	Wavelength		
	Red = 645 nm	Green = 530 nm	Blue = 470 nm
Waist Diameter (μ m)	500 μ m (5cm)	500 μ m (5cm)	500 μ m (5cm)
Sensitivity (V/%RH)	0.0385	0.0249	0.0077
Linearity (%)	98.7420	94.6414	94.5409
Resolution (%RH)	1.299633373	6.53559923	3.111642874

Table 4.10 Characteristics of a U-shaped tapered POF for 500 μ m at all wavelength.

According to the table, a waist diameter of 500 μ m contributes to the highest sensitivity at a wavelength of 645nm with a radius of 5cm. Besides, regarding the resolution, in the context of sensor measurements, refers to the smallest discernible change in the measured variable that a sensor can register. It serves as a quantitative metric representing the precision of the sensor's measurements, indicating its capability to distinguish fine variations. For a refractive index sensor relying on changes in the radius of a U-shaped plastic optical fiber, resolution would denote the minimal shift in refractive index that the sensor can reliably detect. A higher resolution indicates enhanced precision, allowing the sensor to capture nuanced changes in the input variable. This aspect significantly influences the graphical representation of data, ensuring that the plotted graph accurately reflects subtle variations. Attaining optimal resolution involves thoughtful system design, considering potential trade-offs, and requires periodic calibration to maintain accuracy over time. The comprehension

and optimization of resolution are imperative for the sensor to furnish dependable and precise measurements across various applications.

4.2.3 Hysteresis

One of the major parameters used to measure the accuracy of a humidity sensor is hysteresis. The highest difference in observed relative humidity levels during the forward and reverse cycles is defined as hysteresis. Figure 4.7 shows hysteresis for the 500 μm and 600 waist diameter of each light wavelength. It was performed by recording data during forward and reversed measurements. Based on the hysteresis graph for figure 4.7, the output voltage at 55% RH for each wavelength shows a large gap between the forward and reverse processes, which have the lowest ΔV .

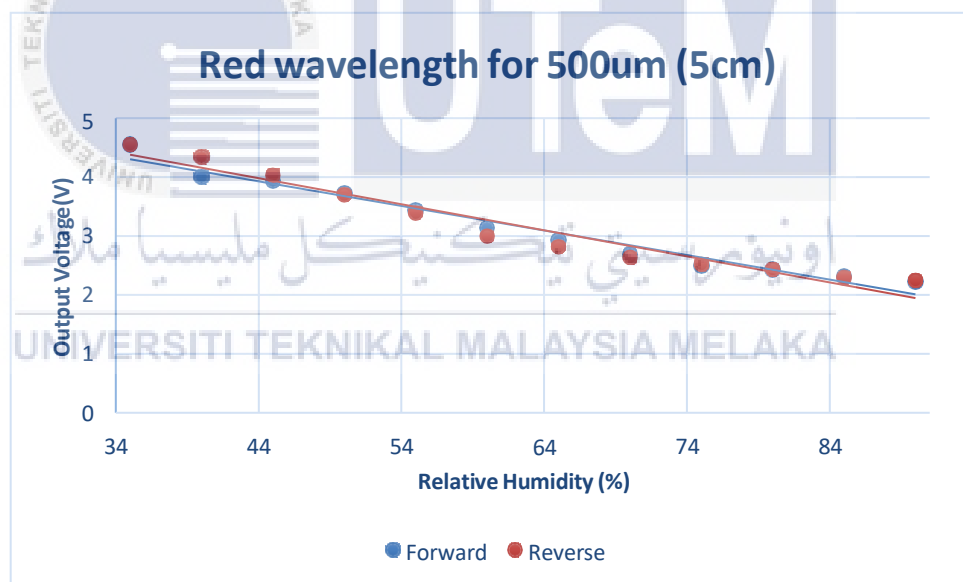
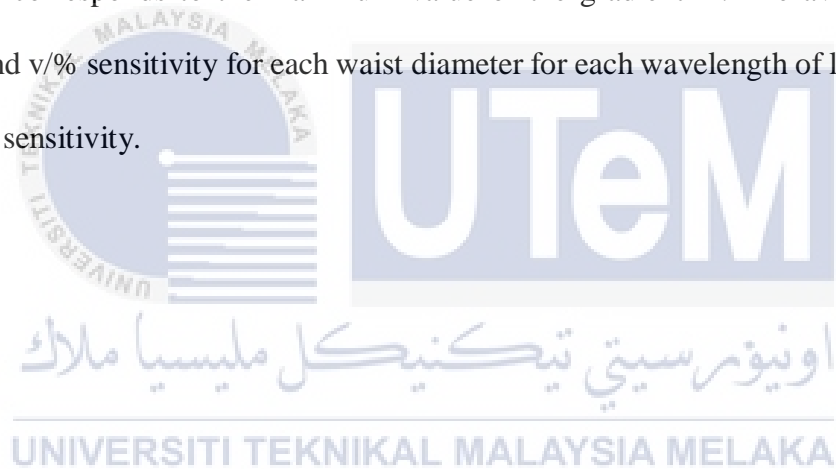


Figure 4.7 Hysteresis for the 500 μm waist diameter of red wavelength

Refer to the graph, it is showing the ΔV for 55% RH is 0.04V. A sensor's low hysteresis results in greater reliability and consistency of measurement.

4.3 Summary

All the graphs in the is inversely proportional to the demonstrate that the output voltage of the U-shaped POF increment of humidity level falls as the relative humidity (%) increases, and that the output voltage of the U-shaped POF increases when the relative humidity (%) declines. The slope-intercept version of a line's equation on a trendline graph is $y = mx + c$, where m is the slope of the line. As a result, the sensitivity of the U-shaped POF sensor corresponds to the maximum value of the gradient m . The average standard deviation and $v\%$ sensitivity for each waist diameter for each wavelength of light determine the greatest sensitivity.



CHAPTER 5

CONCLUSION AND RECOMMENDATIONS

5.1 Conclusion

In conclusion, the study "Development of a Refractive Index Sensor Based on Changes in the Radius of a U-Shaped Plastic Optical Fiber" successfully presents a sensor design and methodology for measuring refractive indices. Using a U-shaped plastic optical Fiber, the researchers demonstrated the ability to detect changes in transmitted light intensity caused by variations in the refractive index of the surrounding humidity. The experimental setup and measurement procedure were carefully designed and executed, ensuring accurate and reliable results. The findings of this study contribute to the field of optical sensing, providing a cost-effective and versatile solution for measuring refractive indices in various vapors concentration. This research opens opportunities for applications in fields such as chemical analysis, biomedical diagnostics, and environmental monitoring. Further developments and optimizations based on this work have the potential to enhance the performance and expand the capabilities of refractive index sensors using plastic optical Fiber.

5.2 Future Works

For future applications, by removing the fiber cladding and coating the core with a higher refractive index material, the plastic optical fibers can be used as the primary ingredient in producing a good sensors for environmental and biomedical monitoring. In addition, to sustain the sensor capability POF can be coated with various of sensitive material for toxic gases sensing application as ammonia, hydrogen sulfide, carbon monoxide and methane.



REFERENCES

- [1] C. Teng, Y. Wang, and L. Yuan, "Polymer optical fibers based surface plasmon resonance sensors and their applications: A review," *Optical Fiber Technology*, vol. 77, May 2023, doi: 10.1016/j.yofte.2023.103256.
- [2] A. J. Y. Tan, S. M. Ng, P. R. Stoddart, and H. S. Chua, "Trends and Applications of U-Shaped Fiber Optic Sensors: A Review," *IEEE Sensors Journal*, vol. 21, no. 1. Institute of Electrical and Electronics Engineers Inc., pp. 120–131, Jan. 01, 2021. doi: 10.1109/JSEN.2020.3014190.
- [3] "Three Basic Components of a Fiber Optic Cable _ by Jo Wang _ Medium".
- [4] C. Teng *et al.*, "Investigation of U-shape tapered plastic optical fibers based surface plasmon resonance sensor for RI sensing," *Optik (Stuttg)*, vol. 251, Feb. 2022, doi: 10.1016/j.ijleo.2021.168461.
- [5] S. Kaur and K. Malik, "Study of Single Mode Fiber (SMF) and Bidirectional fiber cable for various bands of wavelength in optical communication system." [Online]. Available: <https://ssrn.com/abstract=4034864>
- [6] "Advantages and Disadvantages of Fibre optic Cable-GeeksforGeeks <https://www.geeksforgeeks.org/advantages-and-disadvantages-of-fibre-optic-cable/> 2/6 Similar Reads." [Online]. Available: <https://www.geeksforgeeks.org/advantages-and-disadvantages-of-fibre-optic-cable/>
- [7] "Electronic Science Optoelectronics 2. Propagation of light through optical fiber Module 2: Propagation of light through optical fiber."
- [8] "Background & Summary."
- [9] C. G. Danny, M. Danny Raj, and V. V. R. Sai, "Investigating the Refractive Index Sensitivity of U-Bent Fiber Optic Sensors Using Ray Optics," *Journal of Lightwave*

- Technology*, vol. 38, no. 6, pp. 1580–1588, Mar. 2020, doi: 10.1109/JLT.2019.2958044.
- [10] A. Vanderka *et al.*, “Measurement of the optical fiber numeric aperture exposed to thermal and radiation aging,” in *20th Slovak-Czech-Polish Optical Conference on Wave and Quantum Aspects of Contemporary Optics*, SPIE, Dec. 2016, p. 1014224. doi: 10.1117/12.2257339.
- [11] A. Arifin, K. R. Amaliyah, A. K. Lebang, N. Hamrun, S. Dewang, and D. Tahir, “Enhance sensitivity of plastic optical fiber sensor by spiral configuration for body temperature applications,” in *Journal of Physics: Conference Series*, IOP Publishing Ltd, 2021. doi: 10.1088/1742-6596/1811/1/012026.
- [12] J. J. Patil and A. Ghosh, “Intensity Modulation based U shaped Plastic Optical Fiber Refractive Index Sensor,” in *2022 6th International Conference on Trends in Electronics and Informatics, ICOEI 2022 - Proceedings*, Institute of Electrical and Electronics Engineers Inc., 2022, pp. 18–24. doi: 10.1109/ICOEI53556.2022.9776953.
- [13] S. Wang, D. Zhang, Y. Xu, S. Sun, and X. Sun, “Refractive index sensor based on double side-polished u-shaped plastic optical fiber,” *Sensors (Switzerland)*, vol. 20, no. 18. MDPI AG, pp. 1–13, Sep. 02, 2020. doi: 10.3390/s20185253.
- [14] C. Teng *et al.*, “Double-side polished U-shape plastic optical fiber based SPR sensor for the simultaneous measurement of refractive index and temperature,” *Opt Commun*, vol. 525, Dec. 2022, doi: 10.1016/j.optcom.2022.128844.
- [15] Institute of Electrical and Electronics Engineers and IEEE Sensors Council, *IEEE Sensors 2017 : October 29-November 1, 2017, Glasgow, Scotland, UK, Socttish Event Campus (SEC) : 2017 conference proceedings*.

- [16] L. Liu, J. Zheng, S. Deng, L. Yuan, and C. Teng, "Parallel polished plastic optical fiber-based spr sensor for simultaneous measurement of ri and temperature," *IEEE Trans Instrum Meas*, vol. 70, 2021, doi: 10.1109/TIM.2021.3072136.
- [17] J. Filoteo-Razo *et al.*, "U-Shaped Plastic Fiber Optic Sensor for Measuring Adulteration in Liquids via RGB Color Changes," *IEEE Sens Lett*, vol. 5, no. 12, Dec. 2021, doi: 10.1109/LESENS.2021.3128291.
- [18] L. A. Szolga, "Humidity and Isopropyl Alcohol Detection Sensor Based on Plastic Optical Fiber," in *Proceedings of the 2021 25th International Conference Electronics, ELECTRONICS 2021*, Institute of Electrical and Electronics Engineers Inc., Jun. 2021. doi: 10.1109/IEEECONF52705.2021.9467472.
- [19] F. Ye, C. Tian, C. Ma, and Z. F. Zhang, "Fiber optic sensors based on circular and elliptical polymer optical fiber for measuring refractive index of liquids," *Optical Fiber Technology*, vol. 68, Jan. 2022, doi: 10.1016/j.yofte.2021.102812.
- [20] C. Teng *et al.*, "Intensity-modulated polymer optical fiber-based refractive index sensor: A review," *Sensors*, vol. 22, no. 1, MDPI, Jan. 01, 2022. doi: 10.3390/s22010081.

GANTT CHART FOR FINAL YEAR PROJECT 2

ACTIVITY (FYP 1)	WEEK													
	1	2	3	4	5	6	7	8	9	10	11	12	13	14
Meet with supervisor	■	■	■	■	■	■	■	■	■	■	■	■	■	■
Research literature review & gather information		■	■	■	■	■								
Submission of logbook progress						■						■		
Proposal writing	■	■												
Report writing		■	■	■	■	■	■	■	■	■	■	■	■	
Submission of draft report													■	
Submission of report													■	
Preparation for presentation														■
ACTIVITY (FYP 2)	WEEK													
	1	2	3	4	5	6	7	8	9	10	11	12	13	14
Meet with supervisor	■	■	■	■	■	■	■	■	■	■	■	■	■	■
Planning Prototype	■	■	■	■	■	■	■	■	■	■	■	■	■	■
Submission of logbook progress						■						■		
Testing Prototype	■	■	■	■	■	■	■	■	■	■	■	■	■	■
Data Analysis										■	■	■	■	■
Writing chapter 4 and 5										■	■	■	■	■
Submission of draft report													■	
Preparation for presentation														■